Chem Soc Rev

Design of Nanostructures Based on Aromatic Peptide Amphiphiles

Journal:	*Chemical Society Reviews*
Manuscript ID:	CS-REV-07-2014-000247.R1
Article Type:	Review Article
Date Submitted by the Author:	22-Aug-2014
Complete List of Authors:	Fleming, Scott; University of Strathclyde, Department of Chemistry/WestCHEM Ulijn, Rein; The University of Strathclyde, Department of Chemistry/WestCHEM

Cite this: DOI: 10.1039/c0xx00000x

www.rsc.org/xxxxxx

ARTICLE TYPE

Design of Nanostructures Based on Aromatic Peptide Amphiphiles

Scott Fleming[a] and Rein V. Ulijn[a,b]

Received (in XXX, XXX) Xth XXXXXXXXX 20XX, Accepted Xth XXXXXXXXX 20XX
DOI: 10.1039/b000000x

Aromatic peptide amphiphiles are gaining popularity as building blocks for the bottom-up fabrication of nanomaterials, including gels. These materials combine the simplicity of small molecules with the versatility of peptides, with a range of applications proposed in biomedicine, nanotechnology, food science, cosmetics, etc. Despite their simplicity, a wide range of self-assembly behaviours have been described. Due to varying conditions and protocols used, care should be taken when attempting to directly compare results from the literature. In this review, we rationalise the structural features which govern the self-assembly of aromatic peptide amphiphiles by focusing on four segments, (i) the N-terminal aromatic component, (ii) linker segment, (iii) peptide sequence, and (iv) C-terminus. It is clear that the molecular structure of these components significantly influences the self-assembly process and resultant supramolecular architectures. A number of modes of assembly have been proposed, including parallel, antiparallel, and interlocked antiparallel stacking conformations. In addition, the co-assembly arrangements of aromatic peptide amphiphiles are reviewed. Overall, this review elucidates the structural trends and design rules that underpin the field of aromatic peptide amphiphile assembly, paving the way to a more rational design of nanomaterials based on aromatic peptide amphiphiles.

1. Introduction

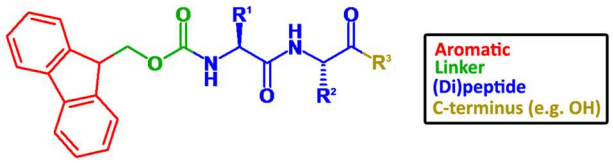

Figure 1 Generic structure of an aromatic peptide amphiphile. Fmoc dipeptide utilised as a typical example.

Supramolecular self-assembly provides a means of achieving "bottom-up" fabrication of nanoscale materials, whereby material properties (e.g. fibrous network topology and stiffness) and functionality (e.g. the bioactivity, electroconductivity) arise from the assembly of relatively simple (e.g. Fig. 1) molecular building blocks.[1–8] Supramolecular materials contrast with traditional covalent polymers, in that assembly is dynamic and reversible, resulting in responsiveness and tuneable characteristics.[9–18] Supramolecular nanostructures, often in the form of hydrogel materials, have various potential applications in areas such as catalysis,[19–24] nanofabrication,[25–28] sensing,[29–32] antimicrobial materials,[33] controlled release and drug delivery,[34–41] and tissue engineering.[42–47]

Self-assembly processes from biological origins can be potentially exploited in the laboratory setting.[48–54] Peptides and peptide derivatives are particularly attractive building blocks for the construction of supramolecular materials – as evidenced by the fact that the apparatus of life itself is largely devoted to the expression of approximately 20 gene encoded amino acids. The expressed polypeptides and proteins undertake an impressive array of structural and functional roles, including molecular recognition, compartmentalisation, catalysis, motility, replication, energy storage, *etc.* While many of these biological structures are too complex to provide scalable technological solutions, minimalistic versions of these systems may give rise to new technologies with properties and functions normally not associated with synthetic materials.

Note that throughout this review, for brevity, peptide sequences will be referred to using their one letter amino acid codes (Fig. 2 lists the 20 gene encoded amino acids). In contrast to their synthetic polymeric counterparts, peptide-based materials offer a rich variety of sides chains which, unlike what is currently possible with synthetic polymers, are organised in a precise sequence that may encompass a range of chemical functionalities and non-covalent bonds.[5,55,15,56–61] For example, a range of charged (D, E, H, R, and K), hydrophilic (S, T, Q, and N), hydrophobic (A, V, L, I, and M), aromatic (F, Y, and W) and other (P, C, and G) residues can all contribute towards the molecular assembly of peptides and proteins, which in turn affects the higher ordered structuring of these molecules.[62–64]

Using insights gleaned from protein structure, synthetic peptides can be designed which contain sequences predisposed to form various supramolecular structures such as α-helix, coiled-coil, β-sheet, collagen and elastin mimics.[15,65–74] It can be advantageous to utilise shorter peptide sequences; where the resultant supramolecular structures are easier to modify.[75,59,76] This allows for a relatively facile chemical synthesis and ultimately easier translation towards real world applications, due to lower costs, scalability, and reduced regulatory barriers in the

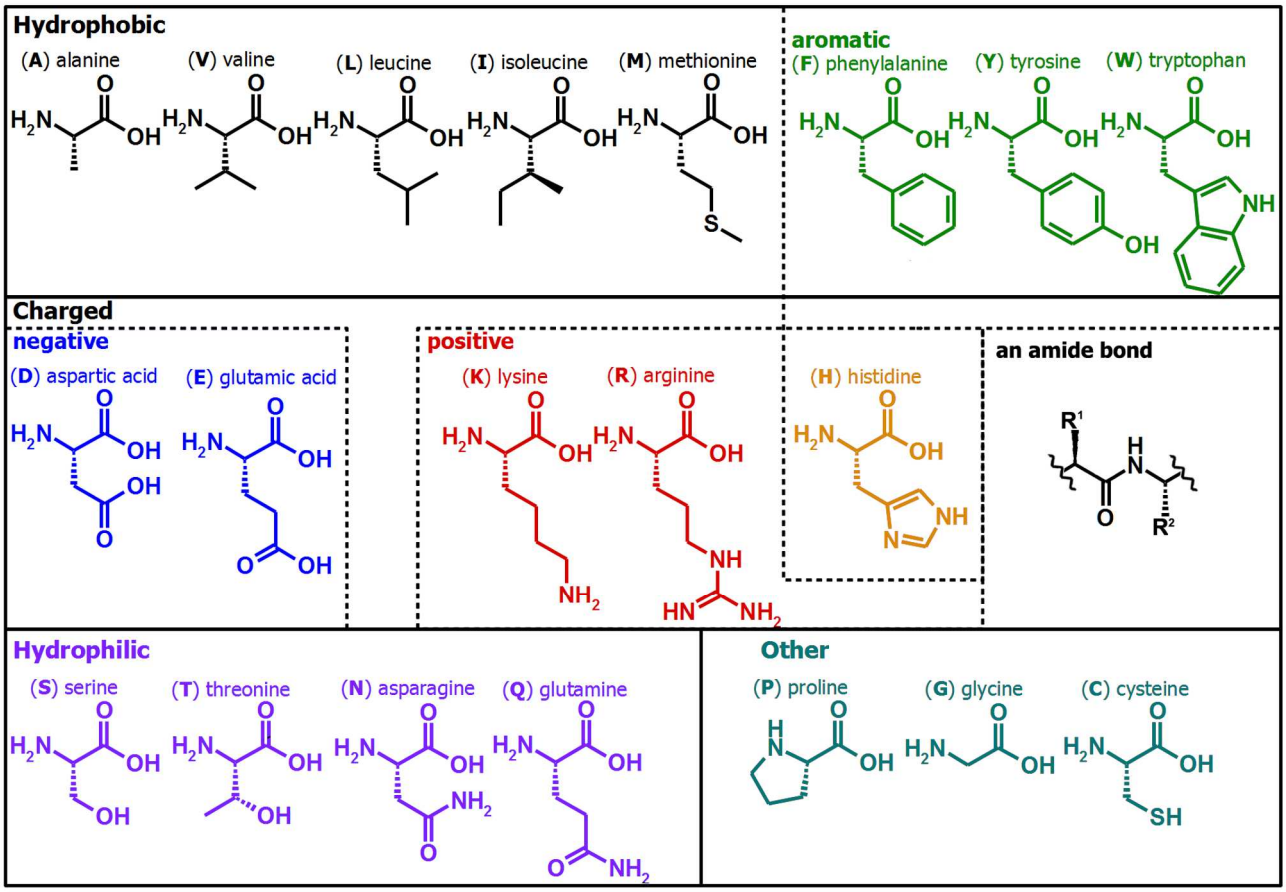

Figure 2 Twenty gene encoded amino acids shared by all life forms.

case of biomedical materials. In addition to numerous literature examples of small molecule (peptide or otherwise) self-assembly motifs,[77–83] structures based upon relatively short peptide sequences often require a synthetic hydrophobic group in order to facilitate self-assembly or gelation.[84–86] To this end, peptide amphiphiles are commonly functionalised with hydrophobic groups such as aliphatic chains.[87,85,88–96,84,97–100] We refer the interested reader to a number of excellent review in this area.[101–104]

An alternative approach is to utilise aromatic functionalities to impart the amphiphilicity required to drive self-assembly – where in this case self-assembly will also be influenced by the directionality associated with the resultant aromatic stacking interactions. This review will provide an overview of the literature relating specifically to the self-assembly and hydrogelation of aromatic peptide (and single amino acid) amphiphiles (Fig. 1) as a separate class of self-assembling peptide systems.

For aromatic peptide amphiphile systems, the peptide component is composed of a short sequence – typically a dipeptide or even a single amino acid – and is capped at the N-terminus with a synthetic aromatic moiety.[57,105–107] The linker segment between N-terminal aromatic and peptide sequence is also a potentially important structural parameter,[108] that has consequences for the relative orientation of the other structural segments. In addition, the C-terminus may also be functionalised,[33,109,110] or is otherwise important for achieving a balance between protonated and ionised forms. Hence, these materials clearly share some of the building block interactions which govern peptide/protein assembly.[66] Despite this, aromatic peptide amphiphiles can be considered as a distinct class of self-assembling materials; in that they adhere to a minimalist design strategy that is facilitated by the inclusion of a synthetic aromatic moiety. For these systems, supramolecular assembly is thought to be governed by a combination of aromatic stacking interactions, and the propensity of the peptide to form a β-sheet-type H-bonding (hydrogen bonding) arrangement.[111–115,42,116] In many cases, this mode of assembly is different from that of aliphatic peptide amphiphiles; whose linear hydrophilic head/hydrophobic tail structure usually predicates the formation of spherical and cylindrical micelles or lamellar structures.[117–123,85,124] In contrast, the self-assembly of aromatic peptide amphiphiles is also influenced by the planarity of aromatic moieties and the geometric restrictions associated with their preferred stacking arrangements.[59,125]

Much work has been carried out in an attempt to rationalise and control, both the self-assembly behaviour and resultant properties of nanostructures formed from aromatic peptide amphiphiles and similar small molecule gelators, *via* the modification of peptide or aromatic components.[126–134] We will consider the impact of molecular structure upon the self-assembly and properties of aromatic peptide (and single amino acid) amphiphile based materials (Fig. 1). In addition, various supramolecular architectures (Fig. 3) that have been proposed in

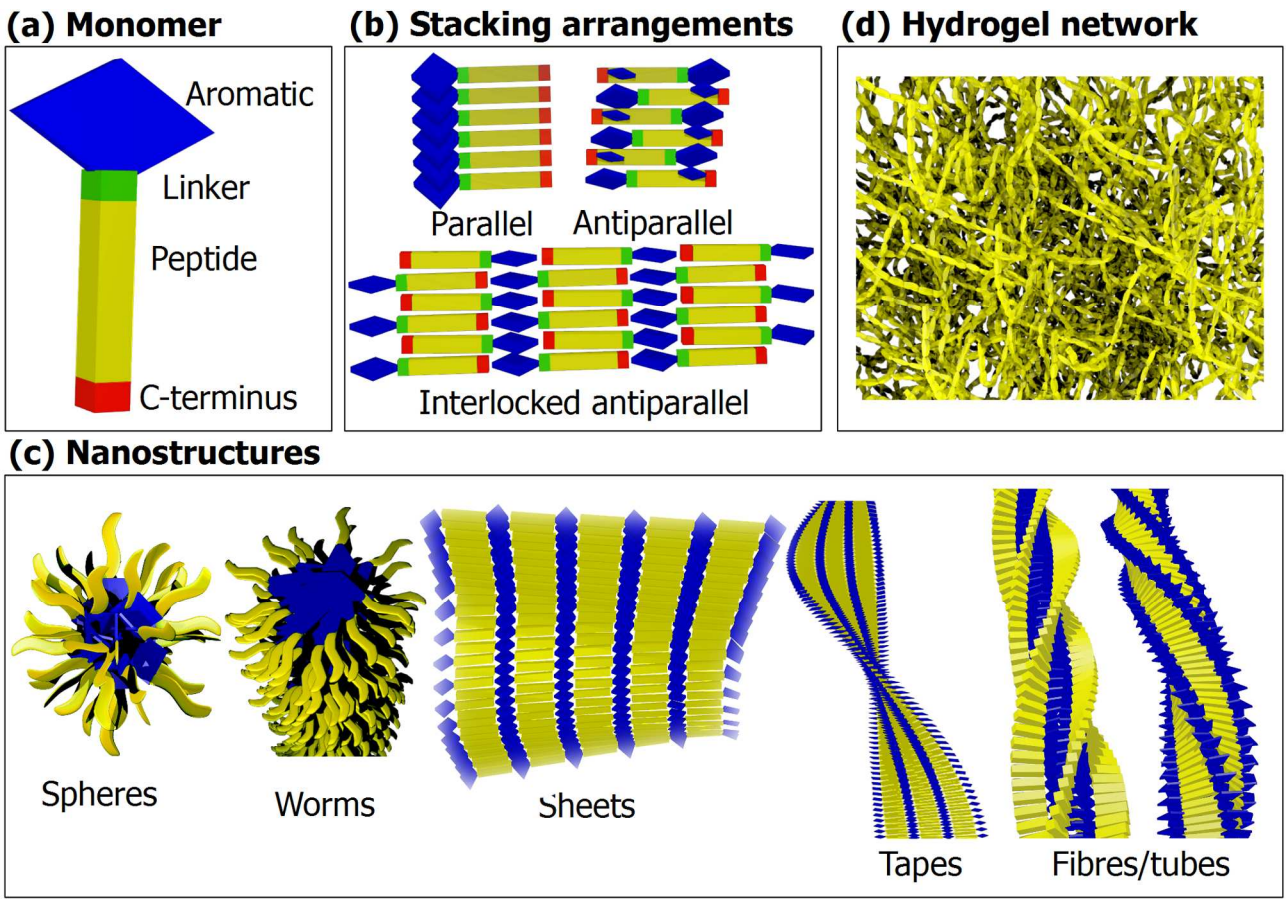

Figure 3 An overview of aromatic peptide amphiphile self-assembly; (a) a simplified aromatic peptide amphiphile; (b) some possible elementary stacking arrangements; (c) supramolecular nanostructures; and (d) a nanofibrous hydrogel network.

the literature will be examined: including the elementary stacking arrangements; chiral nanofibrous architectures; and the formation of worm-like micelles. Self-assembly is also strongly influenced by environmental considerations such as pH, ions, and temperature, and by the kinetic aspects of the gelation process (e.g. for a recent review see[135]). Although important, these aspects of aromatic peptide amphiphile assembly are outside the focus of this review and will not be examined in great detail here.

Various views on the most likely self-assembly mode have been proposed in the literature by our own group and others, and in this respect we have attempted to provide a systematic account of the relevant literature, which we hope will provide a useful reference regarding aromatic peptide amphiphile self-assembly. There is no question that aromatic peptide amphiphiles are increasingly studied and are rapidly becoming an important subset crossing the growing fields of small molecule and peptide self-assembly.

2. Aromatic peptide amphiphiles: A historic perspective

The first known example of an aromatic peptide amphiphile hydrogelator was reported in 1995 by Vegners, where Fmoc-LD was found to form a thermoreversible gel after a heat-cool cycle.[136] This gel was used as a carrier (or *adjuvant*) for the delivery and presentation of antigens, with the loaded material successfully eliciting an antibody response when injected into rabbits. However, it was not until 2003 onwards that a variety of Fmoc (9-fluorenylmethoxycarbonyl) dipeptide hydrogels were

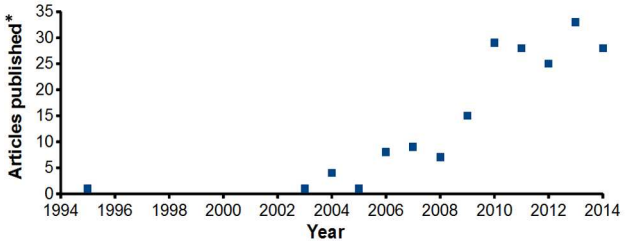

Figure 4 Timeline showing the prominence of aromatic peptide amphiphiles in the literature. *As of July 2014; this is unlikely to be exhaustive since field has lacked specific terminology, but it does illustrate the lag period and growth following initial work byVegners.[136]

serendipitously rediscovered by Xu,[36,137] *en-route* to a subsequently reported pyrenyl analogue.[138] In addition, Xu reported the first enzyme triggered self-assembly of an Fmoc amino acid, whereby hydrogelation was initiated via cleavage of a pendant phosphate group to form the gelator Fmoc-Y *in situ*.[139,30]

Concurrently, Gazit's group demonstrated the role of aromatic amino acids in the formation of amyloid structures, and through a reductionist approach identified diphenylalanine (FF) as a minimal sequence to form peptide nanostructures.[140–148] Recently, it was described that phenylalanine itself is also able to undergo

molecular self-assembly.[149] FF is also able to form peptide nanotubes on account of the directionality offered by a combination of H-bonding and repeated phenyl stacking interactions.[150,151,26,152] The addition of various N and C-terminal capping groups – to investigate the possible role of electrostatic interactions in the FF assembly process – resulted in the discovery of the now ubiquitous Fmoc-FF.[153] This initial work on diphenylalanine based nanostructures led to the approximately simultaneous, but independent, discovery of physiologically stable hydrogels based on Fmoc-FF by our group[154] and Gazit[37] for use in cell culture, thus opening up potential applications within a biological and biomedical context. In 2006 a variety of further aromatic peptide amphiphile hydrogelator studies were published,[155,156,45,157,158] and since then the field has continued to grow (Fig. 4); 2007,[159,160,31,130,44] 2008,[161,162,29,163,164,57,165] 2009,[166–168,34,43,35,169–172,133,115,3,42] 2010,[173,27,174–177,21,178–186,25,187,114,33,128,112,131,105,132,111,4] 2011,[188–191,46,192–197,28,198–200,127,126,9,86,134,110,109,201,202] 2012,[203,19,204–215,129,113,10] 2013,[216–230,116,135,231,23,232–236,22,237,238] and 2014.[18,24,39–41,47,239–260]

3. Aromatic peptide amphiphiles: The four segments

The structures of aromatic peptide amphiphiles can be broken down into four key segments; the N-terminal aromatic, linker, peptide sequence, and the C-termini. These structural facets are of course interlinked, and as a consequence, deconvoluting their relative influence upon the self-assembly process is a challenge. Nevertheless, we will show that a systematic approach gives rise to some general insights into design, so this section aims to provide the reader with an appreciation of the structural diversity available when attempting to tailor aromatic peptide amphiphile systems.

3.1 The N-terminal aromatic moiety

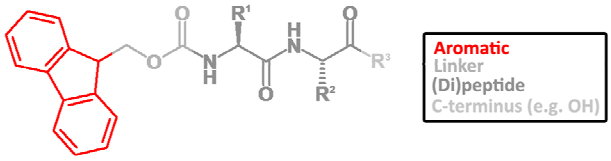

Figure 5 Generic structure of an aromatic peptide amphiphile with the aromatic moiety highlighted.

Self-assembling peptide hydrogels featuring the Fmoc moiety are commonplace; due to its use as a protecting group in peptide synthesis. Fmoc has been found to assist the self-assembly process and facilitate gelation for a number of systems.[232,86,234] For example, various phenylalanine and tyrosine derivatives have demonstrated that (unlike Fmoc) an N-terminal Cbz (carboxybenzyl) group is not found to be conducive to hydrogelation.[180] However, this is dependant upon the corresponding peptide sequence and/or C-terminus; with a Cbz-FF hydrogel and various other examples reported.[159,239] The importance of aromatic stacking interactions has also been illustrated for a series of dipeptide and amino acid based derivatives, where the aromatic Fmoc group at the N-terminus has also been found to be a more consistent facilitator of gelation when compared to a simple hydrophobic group such as Boc (tert-butoxycarbonyl) – indicating that specific aromatic stacking interactions are important.[33]

Given that the N-terminal aromatic moiety is the key design aspect that differentiates aromatic peptide amphiphiles from other self-assembling peptide systems, it is unsurprising that a variety of synthetic aromatic moieties – besides Fmoc – have been utilised to augment the hydrogelation or to introduce functionality, such as charge transfer or electroconductivity, into these systems. To this end, various aromatic moieties have been utilised at the N-terminus such as phenyl, naphthalene, azobenzene and pyrene derivatives.[138,248] The various linkers, substitutions and peptide sequences associated with alternative aromatic functionalities make a systematic comparison of these ligands impractical (Fig. 6).

For instance, pyrene based peptide amphiphile hydrogelators have been studied which utilise less hydrophobic sequences such as AA (e.g. as opposed to FF).[138] Furthermore, the VYGGG pentapeptide sequence is found to be too hydrophobic for achieving hydrogelation (or indeed dissolution) when used in conjunction with an N-terminal pyrene moiety, whereas similar Fmoc and naphthalene compounds do form hydrogels.[179] Other pyrene based amino acid (A, F, W) amphiphiles have utilised a hydrophilic 3-(dimethylamino)-1-propylamine C-termini modification (see Section 3.4), and exhibit an ability to gel in a variety of organic solvents in addition to water.[240] Although some general conclusions may be drawn on the basis of the relative hydrophobicities, there is currently no obvious means of predicting the appropriate peptide sequence for a given N-terminal aromatic functionality. However, known examples suggest that the hydrophobicity of the aromatic component can be offset by the properties of the corresponding peptide sequence or C-terminus.

A study has suggested that in some cases naphthalene can be preferential to Fmoc, e.g. as defined by the respective minimum gelation concentrations of analogous compounds.[126] Peptide amphiphiles capped with an N-terminal naphthalene functionality have also been shown to form (inter/intra)cellular nanofibres – a process with potential anti-cancer applications.[244,227,260–262] Furthermore, the self-assembly properties of naphthalene based systems have been augmented *via* nitrile or bromo substitutions on the aromatic system,[128] with the electron-withdrawing nature of the bromo and nitro groups reducing the electron density of the π-system, which consequently is likely to have an impact on the aromatic stacking interactions and the overall self-assembly structure.

Hence, ring substitutions are another potential variable to consider – particularly for introducing complementary aromatic stacking interactions. These types of modifications also provide a means of altering the hydrophobicity of the molecule – with consequences for the critical gelation pH which is related to the hydrophobicity of a given gelator (see Section 3.4.1). For example, various derivatives possessing a penta-fluorinated N-terminal phenyl moiety have been shown to form hydrogels, whereas analogous non-fluorinated compounds failed to do so.[241] Here, self-assembly is believed to be facilitated *via* quadrupole-quadrupole interactions between aromatic amino acid side chains and the fluorinated N-terminal functionality. In addition, on the basis of computational results quadrupole-dipole-quadrupole interactions – which utilise a sandwiched water molecule – may

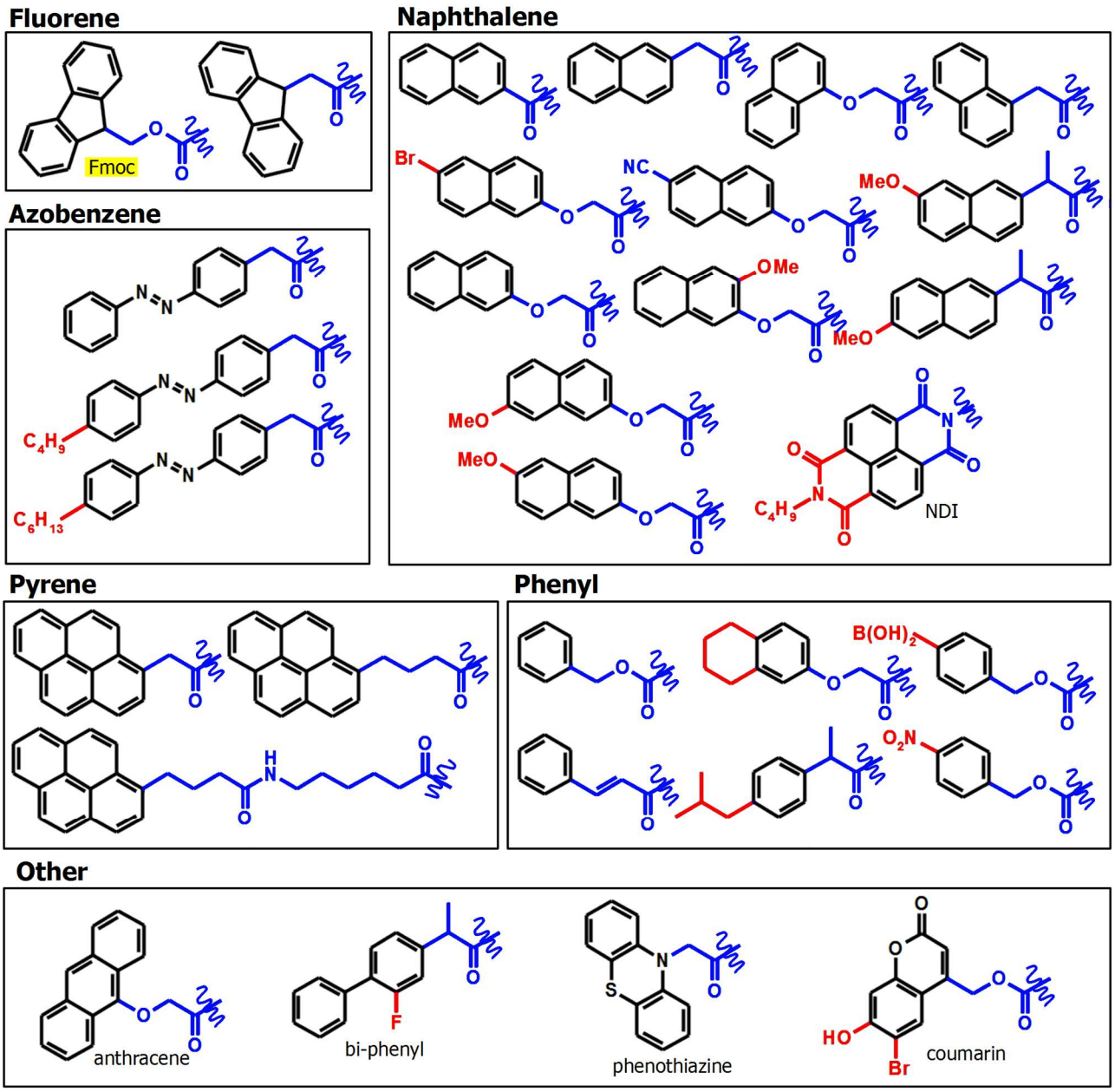

Figure 6 A selection of aromatic moieties and linkers reported in the literature classified according to structure. Red indicates a substituent not part of the core aromatic functionality, whilst blue indicates the linker that connects to the N-terminus of a peptide sequence.

also contribute towards the hydrogelation process.

The aromatic group may in itself also have a functional role, in addition to being a structural motif incorporated to facilitate self-assembly. For example, azobenzene has been exploited due to the cis/trans conformational switches that are mediated under UV (ultraviolet) irradiation.[199] Using this mechanism it is possible to induce reversible photo-responsive gel-solution transitions.[134,250] In addition a change in the azobezene conformation has been observed to initiate a morphological change in the fibres associated with a diglycine derivative.[196] Furthermore, a recent example utilises dithienylethene peptide derivatives, whereby ring opening and closing can be reversibly achieved by applying 312 and 500 nm irradiation, respectively.[242] This dithienylethene ring opening/closing mechanism results in corresponding spectroscopic (colour) changes in the hydrogel samples. Other stimuli responsive systems have also been demonstrated using a range of cleavable aromatic moieties. For example, gel to solution transitions can be initiated using oxidative, reductive or photolytic cleavages of respective BPmoc (para-borono-phenylmethoxycarbonyl), NPmoc (para-nitro-phenylmethoxycarbonyl) or Bhcmoc (6-bromo-7-hydroxycoumarin-4-ylmethoxycarbonyl) functionalities.[193]

Nucleobases have also been utilised as novel N-termini for aromatic peptide amphiphiles.[263,264] Adenine, thymine, guanine, and cytosine based hydrogelators have all been reported. Although trends are difficult to elucidate, like-for-like examples based on either purine or pyrimidine heterocycles appear to commonly gel at similar pH values.[265,266] Moreover, purine

examples that exhibit larger elastic moduli than their pyrimidine counterparts have been suggested to possess increased aromatic stacking interactions.[50] However, similar to other examples, the ability of a given nucleobase derived molecule to undergo hydrogelation is sensitive to peptide sequence and chirality.[267] Overall this is an interesting approach, which in addition to aromatic stacking interactions, also allows for potential base pairing between suitable hydrogelator molecules.[268,50]

Through the co-assembly of molecules bearing different aromatic moieties, it is possible to incorporate a variety of aromatic groups in a single system – a strategy that can help stabilise aromatic stacking interactions *via* complementary interactions. In this way intermolecular energy transfer mechanisms can be observed between the respective fluorophores.[269–272] For instance, a dansyl acceptor/naphthalene donor system has been demonstrated, whereby the naphthalene-diphenylalanine derivative forms fibres based partly on aromatic stacking interactions, with the dansyl component intercalating within this construct (Fig. 7).[175] In addition, this study also showed an energy transfer mechanism between co-gelating peptide amphiphiles, with naphthalene continuing to act as a donor to an anthracene based amphiphile acceptor. In both cases, energy transfer is shown by a redshift in the fluorescence emission and the corresponding quenching of the emission associated with the donor species.

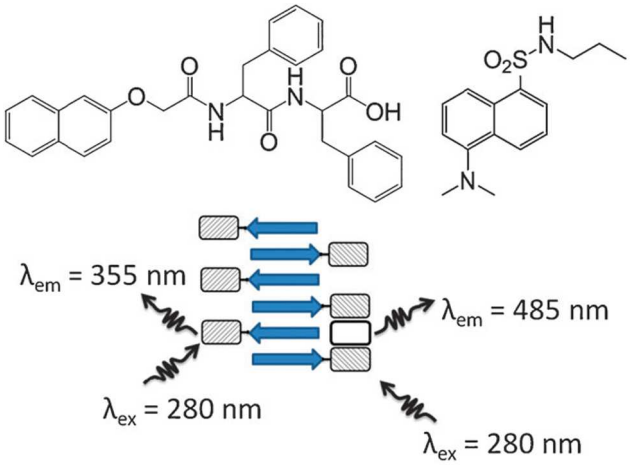

Figure 7 (left) Naphthoxymethyl-FF; (right) dansyl derivative; (bottom) depiction of the energy transfer mechanism *via* the intercalation of dansyl within the assembly. Adapted from Ref. [175] with permission from The Royal Society of Chemistry.

Functional aromatic intercalation has recently been demonstrated using a DCL (dynamic combinatorial library)[273–278] approach that incorporated a dansyl derivative acceptor, which intercalates with a naphthalene donor based peptide amphiphile.[218] In this case, the enzyme thermolysin mediated the selection of gelator candidates *via* a reversible peptide coupling process, in order to attain the most thermodynamically favourable hydrogel system, where free energy of the gelation process drives the reaction. Here, the enzymatic conversion to yield the YF sequence was seen to increase with the inclusion of the dansyl derivative. Similarly, enzymatic conversion towards an NDI-YF hydrogelator has been seen to be enhanced by the addition of a di-alkoxy/hydroxy–naphthalene donor molecule.[243] Hence, these examples demonstrate that the inclusion of an appropriate acceptor/donor molecule can potentially increase the aromatic stacking interactions within the nanostructure, improve the stability of an existing hydrogel system, and possibly attain materials with some degree of electroconductivity.[185]

3.2 The linker segment

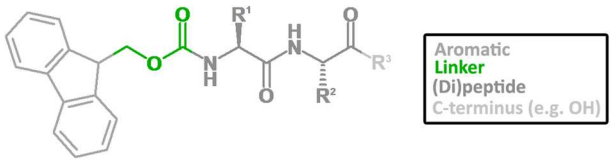

Figure 8 Generic structure of an aromatic peptide amphiphile with the linker segment highlighted.

The choice of linker (see Section 3.1, Fig. 6 for examples) between the aromatic and peptide component is also vital to achieving hydrogelation of these materials. For example, while the naphthoxy group promotes gelation, equivalent naphthalene based amphiphiles with alternative linkers fail to form hydrogels.[130] These observations have been rationalised to some extent by molecular modelling of the angles between the various linkers (Fig. 9). With increased curvature of the energy minimised state associated with the molecules found to be detrimental to effective assembly. Here, gelators seem to require relatively linear geometries in order to allow effective intermolecular interactions in both the aromatic and peptide self-assembly domains. In addition, the fact that the methoxy linker is a potential H-bond acceptor may also have implications for self-assembly.

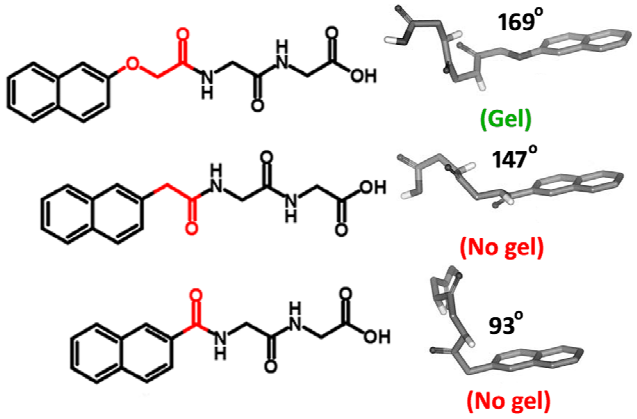

Figure 9 The effect of the linker on the overall molecular geometry; with a relatively linear conformation being optimal for gelation. Adapted from Ref. [130] with permission from The Royal Society of Chemistry.

Another recent study has also shown the utility of the methoxy linker associated with the Fmoc moiety in comparison to analogous alkyl fluorenyl linkers.[108] Here, both the linker length and flexibility are proposed to be important; with the carbamate moiety of Fmoc providing a relatively rigid fluorenyl conformation for robust aromatic stacking and H-bonding interactions – as indicated by an increased rotational energy barrier associated with the carbamate compared to the otherwise equivalent ethylcarbonyl linker. Fortuitously, the convenient Fmoc moiety appears to be a relatively good choice for aromatic peptide amphiphile hydrogelators – as defined by the gelation pH

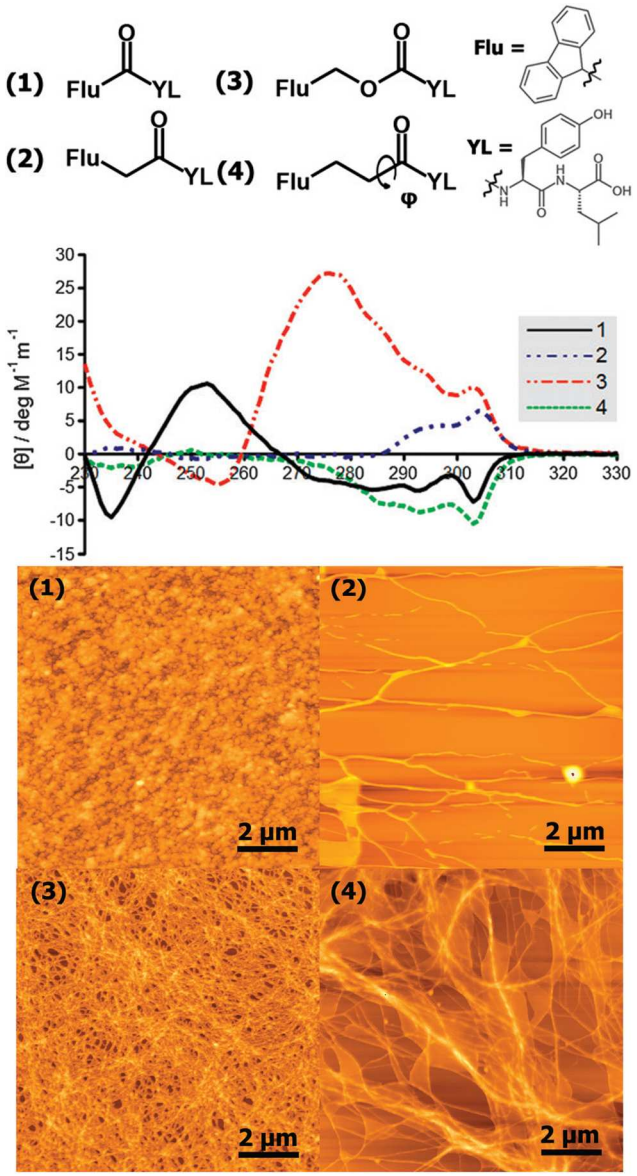

Figure 10 Effect of various linkers upon the observed circular dichroism handedness and AFM network morphologies associated with fluorenyl YL derivatives. Adapted from Ref. [108] with permission from The Royal Society of Chemistry.

and rheological properties compared to the alternative linkers in this study. The choice of linker also markedly influences both fluorescence emission and FTIR (Fourier transform infrared) spectra – with some linkers resulting in reduced aromatic stacking interactions and/or H-bonding disruption, presumably due to restrictions in the available molecular orientations. In addition, the number of methylene units was found to alter the handedness of the observed supramolecular chirality by CD (circular dichroism) (Fig. 10). These results mirror similar findings for aromatic-steroidal based organogelator systems, where an odd or even number of methylene units in an analogous linker segment influenced the gelation properties.[83,279] Although not directly related to aromatic peptide amphiphiles, this work also highlights the impact this region of the gelator can have on supramolecular chirality and the consequent self-assembly process. Hence, the linker clearly influences the conformations available to the gelator molecules, and as such the optimal linker is likely to depend upon the aromatic group and peptide sequence in question. Unfortunately, although aromatic peptide amphiphiles have generally utilised a variety of linkers, side-by-side comparisons in the literature are rare – we propose this should be a more active area of research.

3.3 The peptide sequence

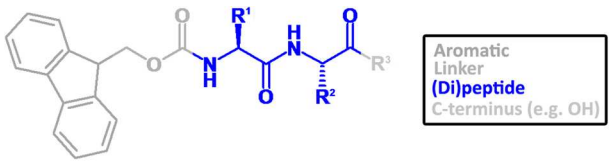

Figure 11 Generic structure of an aromatic peptide amphiphile with the peptide sequence highlighted.

3.3.1 Amino acids

There are twenty gene encoded amino acids across all living systems (Section 1, Fig. 2), with a further set formed by post translational modification. An increasing number of non-natural amino acids (currently several hundred) are also available. Amino acids can be broadly classified in terms of their relative affinity for water, based on whether they possess hydrophobic or hydrophilic side chains.[280,281] For instance, aromatic residues such as F or Y and aliphatic residues such as V or L are classed as hydrophobic. In addition, there are five amino acids that are charged at physiological pH, which possess either an acidic (E and D) or basic (H, R, and K) side chain – similarly these are also hydrophilic. Furthermore, there are three special amino acids: G the most flexible and the only non-chiral amino acid; P whose rigidity in conjunction with glycine's flexibility is important in forming beta turns (within a protein context);[282] and C which can be readily oxidised to form disulfide bonds.[283,184]

3.3.2 The assembly of peptide fragments

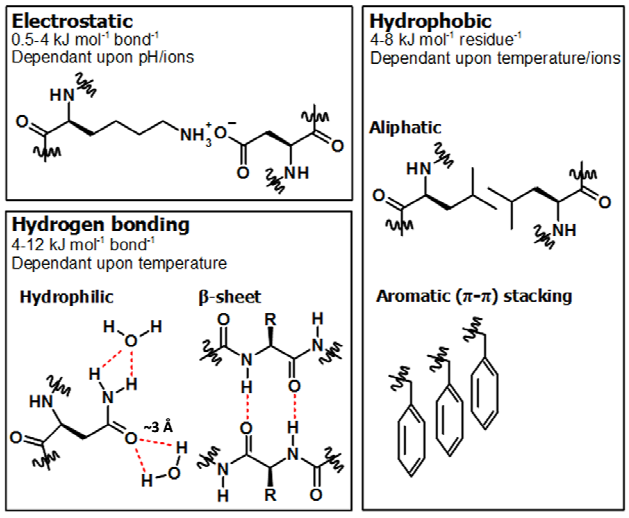

Figure 12 Summary of non-covalent interactions (and corresponding energies[284]) associated with peptides.

Various intermolecular interactions (Fig. 12) are possible depending upon the amino acid sequence, such as electrostatics,[285] hydrogen bonding, aromatic stacking, and van der Waals forces. In aqueous self-assembly, the influence of any permanent dipoles or charges associated with the gelator will be

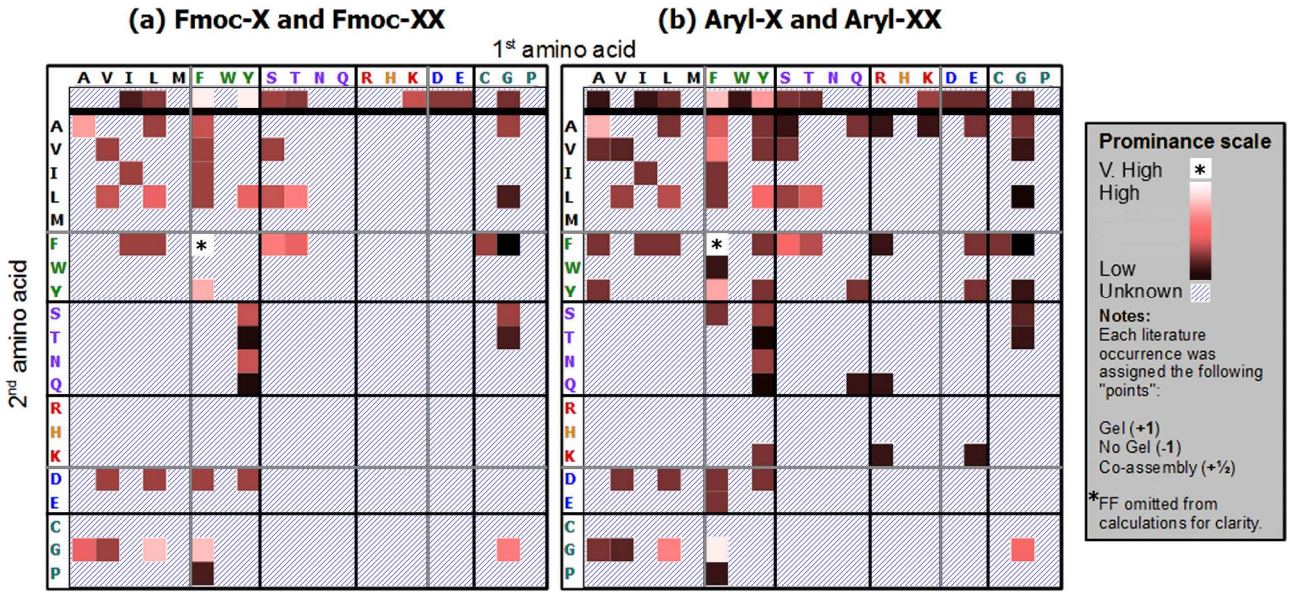

Figure 13 Literature/self-assembly prominence summary for all natural amino acid and dipeptides (respectively separated by thick black horizontal lines) as pertaining to (a) Fmoc and (b) N-terminal aromatics in general. Thin black lines define hydrophobic, hydrophilic, charged, and other side chain classifications. Thin grey lines define subcategories (as far as reasonably possible) – i.e. aliphatic/aromatic and positive/negative.

diminished through H-bonding with water and electrostatic interactions with any dissolved ions. Hence, although the relative importance of the respective intermolecular interactions varies, for hydrogel materials it is the hydrophobic interactions which dominate the self-assembly process.

The importance of hydrophobic interactions in the assembly of short peptides has also been elucidated through extensive work on the amyloid formation of peptide fragments (e.g. FF) in an effort to deduce some of the possible mechanisms in protein misfolding diseases such as Alzheimer's.[140,141] This work revealed that aromatic interactions are the dominant contributor towards amyloid formation, with H-bonding interactions also a significant factor. Furthermore, the propensity of hydrophobic – and in particular aromatic – residues to effect the self-assembly of short peptides, has also been previously revealed in a computational study of all 400 natural dipeptide combinations.[286] Although these amyloid and computational dipeptide systems are evidently not aromatic peptide amphiphiles, this comprehensive assessment of the self assembly of all possible dipeptide motifs provides useful insights, which are also relevant to aromatic peptide amphiphile assembly. Hence, the apparent predominance of aromatic residues (Fig. 13) in literature examples[164] of aromatic peptide amphiphiles should come as no surprise.

3.3.3 General sequence space trends

Figure 13 summarises the relative prominence of the 20 amino acid and 400 natural dipeptide sequences for (a) Fmoc and (b) aromatic peptide amphiphiles in general, in terms of both literature occurrences and reported material properties (e.g. gel or no gel).The choice of peptide sequence is of course paramount to the self-assembly and gelation ability of aromatic peptide amphiphiles. Ultimately, for effective gelation a hydrophobic/hydrophilic balance must be reached where aggregation is favoured, but precipitation does not take place. However, whilst these general principles are understood, designing novel gelators, and rationalising their behaviour, remains a challenge.[287]

A systematic comparison of the experimentally observed gelation ability of aromatic peptide amphiphiles based upon their amino acid or dipeptide sequence is difficult. This is in part because the gel state often represents a kinetically trapped, route dependant,[135] non-equilibrium state, so many different meta stable structures may be formed from any particular gelator molecule, depending on the route of gelation. Indeed, different authors almost invariably follow different gelation protocols.[135,210,288] In addition, environmental conditions such as pH,[127,289,171] the gelator concentration, and the presence of ions,[190,216,212,211] also inevitably influences the self-assembly properties of a given aromatic peptide amphiphile system. However, despite these difficulties in making direct comparisons, a literature analysis of Fmoc (Fig. 13 (a)) and more generally aromatic (Fig. 13 (b)) peptide amphiphiles, highlights the importance of hydrophobic and in particular aromatic residues in terms of self-assembly and gelation capability (note that for the purposes of Fig. 13, only gene-encoded α amino acids were considered).

However, there is also clearly a historic bias from Gazit's pioneering work, and the role of diphenylalanine in amyloid formation as described above, making it a natural first choice for many novel hydrogelators,[52,140,96,25,26,290,146] Nonetheless, the emphasis on aromatics indicates that the presence of aromatic amino acids can facilitate the gelation process through aromatic stacking interactions,[187] which may act to reinforce the H-bonded β-sheet type arrangement.[164] Furthermore, it has been found that for a wide variety of naphthalene and Fmoc dipeptides, there is a correlation between the ClogP (calculated partition coefficient) values, and the minimum gelation concentration and/or highest gelation pH.[128,131] Although it should be noted that this rule does not hold for all sequences, e.g. Fmoc-FG and Fmoc-LG behave as expected, but equally hydrophobic Fmoc-GF and Fmoc-GL do not show gelation.[289,127] There are also kinetic effects, with

increasing aromatic residues in the peptide backbone found to increase the rate of hydrogelation and the stiffness/elasticity of the network formed.[113,133]

Although general trends can be observed with respect to the hydrophobicity/aromaticity associated with the peptide sequence and the corresponding physical properties of the resultant systems; it is currently not possible to reliably predict whether a given molecule will form a hydrogel solely on the basis of ClogP values alone. In this respect, some notable outliers do exist; unsurprisingly the minimalistic diglycine (GG) sequence has been the subject of several studies.[127,130,131,36,196] There are also examples of successful aromatic peptide amphiphile gelator systems, which also feature hydrophilic and/or charged residues such as S, T, Q, N, and E.[204,189] These are invariably combined with hydrophobic amino acids F or Y, with hydrophilic-hydrophilic examples being of low prominence or otherwise unknown. Hence, despite the fact that large areas of the dipeptide space remains apparently unexplored, there is clearly significant scope for covering the entire range of amino acids and dipeptides.

3.3.4 Short sequences, large impact

Relatively small changes to the molecular structure can have a large impact upon the self-assembly, gelation, and properties of these materials.[249] Fmoc-Y and Fmoc-F hydrogels differ only by an –OH group, yet substantial rheological differences are observed.[172] Whilst the elastic and viscous moduli of Fmoc-Y are observed to be largely independent of the applied frequency, Fmoc-F exhibits moduli that are heavily influenced by the frequency. In addition, encapsulated dyes are released more easily from the Fmoc-F hydrogel. This suggests that Fmoc-F forms a more flexible network, which adapts to applied mechanical stresses. Whereas Fmoc-Y is a significantly stronger gelator; presumably the additional H-bonding donor has an impact upon the H-bonding arrangement and the precise supramolecular orientation adopted. Other hydrogel systems appear sensitive to the sequence order, since upon the inversion of an Fmoc-VLK(Boc) sequence, Fmoc-K(Boc)LV exhibits relatively unoriented assemblies, branched fibres and a larger elastic modulus.[177]

It is also possible to augment supramolecular materials with covalent disulfide linkages. For example, the self-assembled Fmoc-CF-OMe hydrogel can be formed enzymatically in a reducing environment, with subsequent heating resulting in the collapse of the network *via* oxidation of the cysteine residues.[184] Hence, with short peptide sequences it is possible to cover the full range of assembly processes available to natural peptides and proteins. However, compared to a high molecular weight protein or oligopeptide, a single amino acid can evidently have a comparatively large impact upon aromatic peptide amphiphile assembly.

3.3.5 Non-natural amino acid derivatives

It is also possible to alter the peptide component by modifying or replacing naturally occurring amino acids with non-natural derivatives. One approach involves modifying an amenable side chain functionality. For example, in Fmoc-KK(NDI) (naphthalene diimide), a lysine residue is exploited as a pseudo N-terminus in order to introduce aromatic n-type semiconductor functionality.[111] Similarly, in order to achieve an appropriate hydrophobic balance for effective self-assembly and gelation, protecting groups such as Boc may simply be left uncleaved.[177] In addition, non-natural amino acids such as naphthylalanine have been utilised in formation of amyloid based nanostructures,[148] and indeed hydrogels.[133] For example, Fmoc-2-naphthylalanine has been found to exhibit relatively fast hydrogelation on account of the increased aromaticity of its amino acid derivative.[113] Furthermore, taking inspiration from nature, 3,4-dihydroxyphenylalanine (DOPA) has been incorporated into aromatic peptide amphiphiles.[256] The DOPA functionality can thus give rise to hydrogel materials which possess adhesive properties similar to that exhibited by mussels.

In addition, as seen previously with the N-terminal aromatic moieties (Section 3.1), the electronic properties of natural aromatic amino acid residues have been modified *via* various ring substitutions.[235] For example, Fmoc-F has been halogenated with F, Cl, and Br, at ortho, meta, and para positions.[132] In this work, electron deficient side chains are found to enhance the self-assembly rate, illustrating that these single atom modifications have a significant impact on self-assembly and consequent hydrogelation behaviour, with F proving to have the most dramatic effect. Both electronic and steric effects are thought to alter the monomer conformations and the resultant helicity of the fibres, thus resulting in changes to the precise aromatic stacking interactions present within the supramolecular assembly. In addition to mono-halogenated Fmoc-F derivatives, the penta-fluorinated Fmoc-F analogue has also been studied.[109,180] It was found to undergo hydrogelation, and exhibited a reduced gelation concentration compared to Fmoc-Y, whilst Fmoc-F failed to undergo hydrogelation under similar conditions.[180] Electronic, steric, and hydrophobic effects are all believed to be potential contributors to the relative stability of this system. Hence, alteration of the electronics of the aromatic side chains is clearly a useful technique for the tailoring of the structural and physical properties of aromatic peptide amphiphile based materials by enhancing π-stacking interactions between aromatic substituents.[291]

One common strategy to enhance the lifetime of peptide based materials intended for use in biological applications, for example *in vivo*, is the replacement of α with β amino acids. β peptides – such as Nap-βFβF – are less likely to be metabolised due to their increased resistance to proteolytic enzymes.[157] For example, analogous Nap-FFY α and β peptide gelators have demonstrated enhanced biostability associated with the β sequence analogue.[44] In addition, for dipeptide sequences enhanced proteolytic stability can also be imparted by a single β-alanine residue; for instance Fmoc-βAV and Fmoc-βAF are biostable hydrogels for potential *in vivo* drug release devices.[38] Here, the single β-alanine is sufficient to ensure the stability of the amide bond with the natural valine or phenylalanine residue. Alternatively, gelators can utilise the dextro (D-) enantiomers of the natural levo (L-) amino acids. Here, a D-peptide derivative can potentially exhibit host-guest type recognition that not observed with the L-equivalents.[138] In addition, D-amino acid modifications can have consequences for the supramolecular helicity observed by CD.[36] This reversal of handedness can also result in enhanced biostability,[263] as illustrated in a comprehensive study of various Nap-FF derivatives.[35] In this example, α, β, D-, and para fluorinated diphenylalanine Nap-FF gelators were considered for potential drug delivery applications. Only the β and D- variants

were found to exhibit resistance to proteinase K digestion – thus highlighting the utility of these modifications for potential *in vivo* applications necessitating biostability.

3.4 The C-terminus

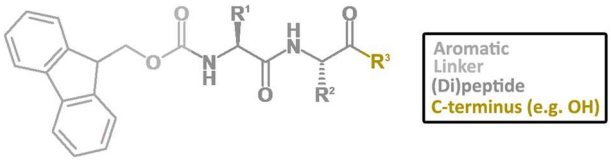

Figure 14 Generic structure of an aromatic peptide amphiphile with the C-terminus highlighted.

For aromatic peptide amphiphiles, which are composed of short (e.g. di- and tri-) peptide sequences, the normally free, acidic, C-terminus, is often vital for achieving a ratio of ionised to neutral gelator molecules conducive to gelation.[171]

3.4.1 pH: controlling the ratio of COOH to COO^-

As previously alluded to, the gelation, properties, and supramolecular structure of a given aromatic peptide amphiphile is usually found to be highly dependant upon the pH of the medium concerned.[210,236] Aromatic peptide amphiphiles, almost invariably, have an associated negative charge from the normally unprotected peptide C-terminus. Hence, altering the pH changes the ratio of acid to conjugate base, which in turn affects the aqueous solubility of the system. Ultimately it is the solubility and charge associated with the aromatic peptide amphiphiles that determines whether or not aggregation and gelation is favourable. Therefore it is unsurprising that pH is the primary means of controlling and initiating the gelation of these systems.

Since the assembly of aromatic peptide amphiphiles possessing a terminal carboxylic acid is largely dependant upon the neutralisation of negative charge, one might expect that gelation would only occur at a relatively low pH, below the pK_a of the molecular constituent. However, this is clearly not the case, with many examples of gelation at physiological pH – whilst the typical pK_a for a C-terminal carboxylic acid is approximately 3.5. For example, when pH titration experiments are performed on Fmoc-FF two distinct apparent pK_a shifts are observed corresponding with the onset of gelation and precipitation, respectively.[171] It should be noted that an alternative study reports only a single pK_a associated with Fmoc-FF,[210] this may be due to differences in the precise titration protocol adopted – as the initial Fmoc-FF/pH study used heat-cool cycles between titrations in order to help ensure a minimum was reversibly attained at each pH value. Further studies have shown that Fmoc-FF is apparently unique among closely related systems (FG, GF, GG, LL, LG, GF), which each only exhibit a single apparent pK_a shift under identical experimental conditions.[289,127] The initial Fmoc-FF/pH study[171] reports shifted pK_a values at about pH 9.5 and pH 6.2; which corresponds with the formation of a cloudy gel and the gradual precipitation of Fmoc-FF, respectively. Substantial differences were also observed by FTIR; with decreasing pH initially resulting in the appearance of amide I bands typical of a β-sheet type H-bonding arrangement. At low pH, below the second pK_a, additional FTIR modes also become apparent, presumably corresponding with the formation of precipitate.

Overall this points to a multistep aggregation mechanism with respect to pH (Fig. 15). At high pH, Fmoc-FF is in an ionised and disordered state; below the first shifted pK_a, fibre formation and hydrogelation occurs; fibres continue to aggregate further with decreasing pH and neutralisation of charge; until eventually below the second shifted pK_a precipitation occurs – corresponding with complete phase separation of water and peptide amphiphile. Hence, this illustrates that hydrogelation requires the presence of some remaining ionised material in order to prevent precipitation – the precise ratio required largely depends upon the relative hydrophobicity of the gelator – in line with ClogP correlations.[128,131,127,289] In addition, the observed apparent pK_a shifts show that the self-assembly and gelation process itself acts as a proton sink, which buffers against pH changes while supramolecular reorganisation is proceeding. Although, fibres are often observed at high pH values, the network integrity only increases *via* H-bonding interactions as protonation allows.[112,289,166] Hence, there is likely a distinct supramolecular arrangement associated with aromatic peptide amphiphiles high pH conditions as discussed in Section 4.1.7 below.

3.4.2 C-terminus modifications

As discussed above, the main advantage of using the free acid C-terminus, is that the self-assembly of the gelator can be easily triggered by pH adjustments. However, when the C-terminus is functionalised (Fig. 16) opportunities arise for gels that are stable at a broader range of pH values, as illustrated by Zhimou Yang's example of Fmoc-Y-OMe.[168] For methyl esters, solubility in water can be problematic. Hence, methyl ester functionalised peptide sequences normally possess at least one hydrophilic residue to aid solubility and dispersion in water.[110,129,167] In addition, self-assembly and gelation of these systems is often initiated enzymatically using a condensation reaction of freely soluble amino acid building blocks (often catalysed by the protease thermolysin as discussed in Section 6) or *via* dephosphorylation from a readily soluble precursor. Hence, kinetic aspects which can otherwise hinder the gelation of poorly soluble methyl ester derivatives can be overcome with an *in situ* enzymatic condensation methodology.

A systematic variation of the C-terminus of various side chain halogenated Fmoc-phenylalanine derivatives has broadly revealed that COOH promotes gelation, COOMe promotes precipitation, and $CONH_2$ generally results in solutions.[109] Of course, although these C-termini solubility trends generally hold ($CONH_2$ > COOH > COOMe), depending upon the hydrophobicity of the corresponding N-terminal aromatic and peptide sequence, COOMe[129] and $CONH_2$[218] C-termini can both prove amenable to self assembly and/or gelation. Hence, simple modifications to the C-terminus can have a significant impact on the solubility and consequently the self-assembly characteristics of these materials.

Saccharide modifications have been utilised in dipeptide based hydrogelators.[54] Furthermore, various aromatic saccharide amphiphiles have been shown to also undergo hydrogelation *via* CH-π interactions.[51] Hence, C-termini saccharide modifications have also been used to augment the self-assembly and properties of aromatic peptide amphiphiles.[268] For example, the popular Fmoc-FF motif has been modified with the glucosamine moiety at the C-terminus.[292] In this instance, the saccharide chemical functionality was primarily included for therapeutic reasons – fibrosis inhibition. Given the role that glycoproteins have in

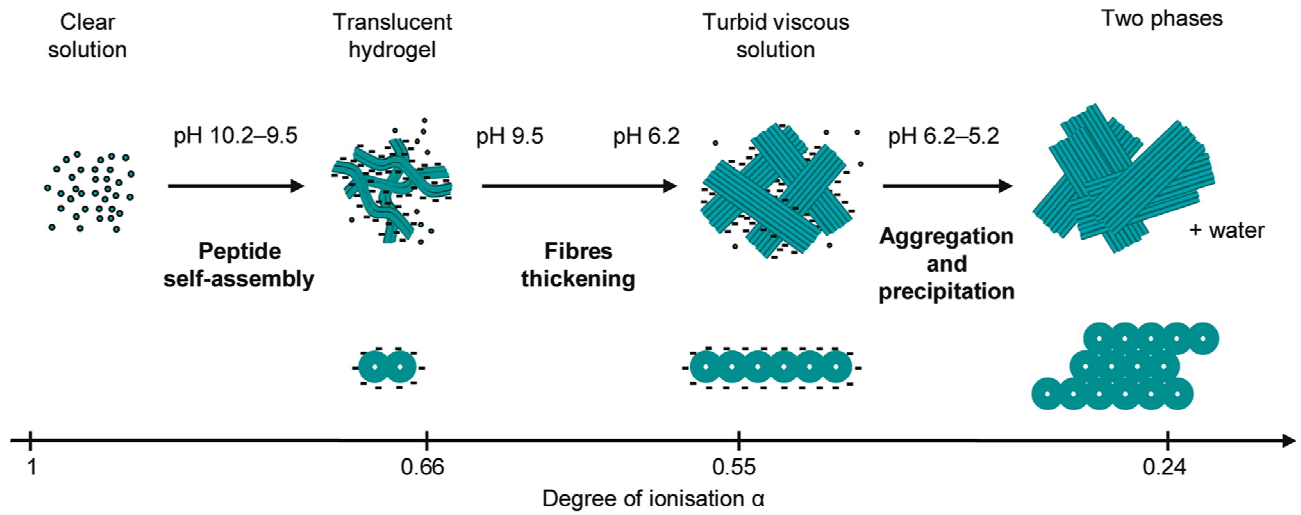

Figure 15 The self-assembly of Fmoc-FF against pH. Reprinted with permission from C. Tang *et al.*, Langmuir, 2009, **25**, 9447–9453.[171] Copyright 2009 American Chemical Society.

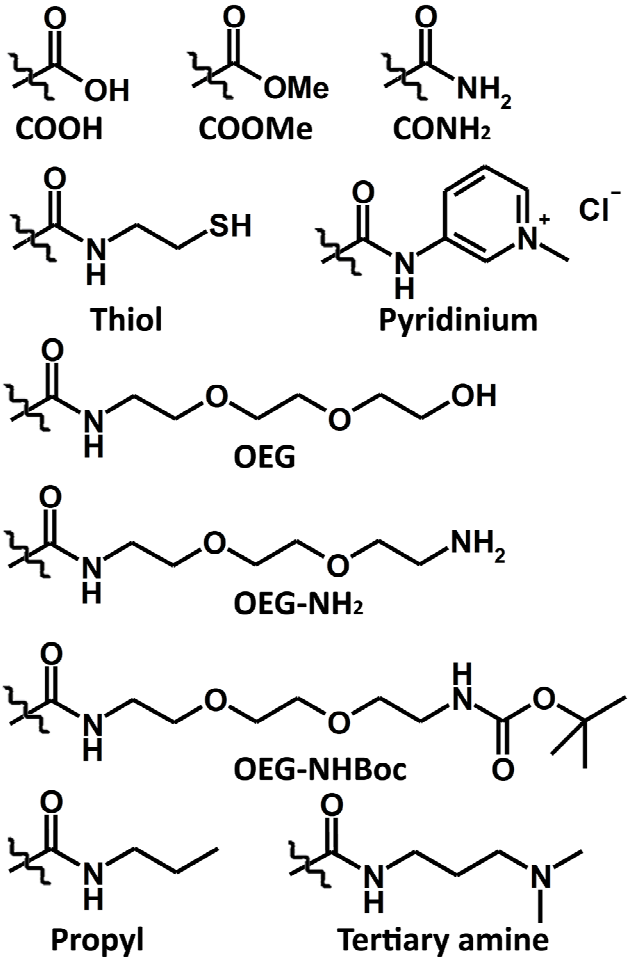

Figure 16 A selection of C-termini reported in the literature. COOH is overwhelmingly the most common of these.

natural cell-cell signalling processes,[264] saccharide modifications are a potentially useful means of altering aromatic peptide amphiphile based biomaterials. In addition, C-termini saccharide modifications have also been employed in order to improve the resistance of aromatic peptide amphiphile materials to proteolysis.[263,266]

Other C-termini used for hydrogelators include a thiol,[31] several pyridinium derivatives,[33] alkyl groups,[239] tertiary amines,[240] and variations of a OEG (oligoethylenegycol) chain.[195,181] The pyridinium and tertiary amine derivatives are of note, since for these systems the C-termini charge has been reversed from negative to positive. Hence, in contrast to the majority of aromatic peptide amphiphiles, these systems become less soluble as the pH is increased. In addition, pyridinium is also of interest due to its antibacterial activity. Unsurprising, the pyridinium gelator with the lowest minimum gelation concentration was based on the familiar Fmoc-FF motif. In addition, one of the OEG based hydrogelator systems,[195] also possesses a cationic C-terminus, Boc protection of which allows for the preparation of organogelators. Hence, there is clearly a lot of scope for augmenting or altering the self-assembly properties of aromatic peptide amphiphile materials *via* modification of the C-terminus. Ultimately the hydrophobicity of the corresponding aromatic and peptide components must be suited to a given C-terminus for hydrogelation to take place.

4. Supramolecular organisation

The supramolecular organisation of aromatic peptide amphiphiles can be considered to consist of two hierarchical self-assembly arrangements; molecular stacking conformations and the mechanisms that usually favour one dimensional growth. Whilst there are clearly many parallels betweeen protein and aromatic peptide amphiphile assembly, secondary structure derived terminologies can be confusing within this context. Hence, throughout this review secondary structure terms are utilised only as a conveniant analogy, and should not be interpreted literally. It should also be noted from the outset; that since radically different structures can be obtained from closely related gelators, a single supramolecular self-assembly paradigm, which is representative of all aromatic peptide amphiphile systems, is unlikely.

4.1 Possible stacking conformations

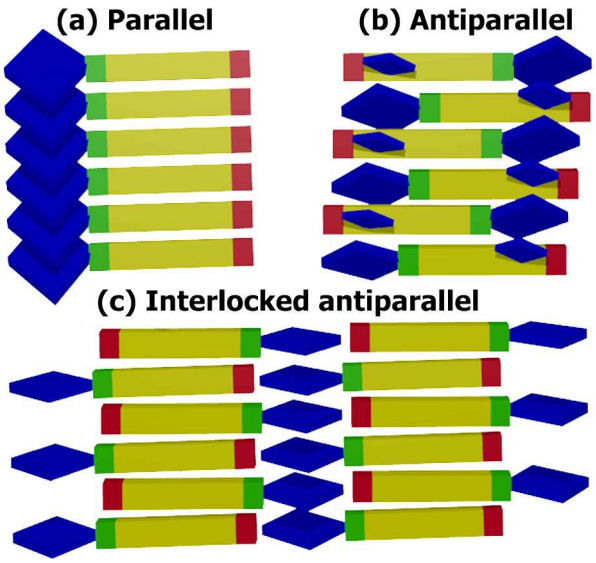

Figure 17 Depiction of possible aromatic stacking interactions present in aromatic peptide amphiphile nanostructures: blue diamonds represent the N-terminal aromatic moiety; cuboids represent the dipeptide sequence, and the small blue squares in (b) correspond to aromatic side chains.

The self-assembly of aromatic peptide amphiphiles is based upon the alignment of relatively hydrophobic and relatively hydrophilic regions of the molecules.[31] For aromatic peptide amphiphiles, hydrophobic contributions are dominated by the influence of the aromatic functionality at the N-terminus, whereas the peptidic H-bonding arrangement assumes the role of the relatively hydrophilic motif. One of the key questions associated with this supramolecular stacking arrangement is whether a parallel or an antiparallel stacking conformation is adopted, with evidence for both modes of assembly presented in the literature. In addition, less organised structures, typically observed with systems that have an imbalance in hydrophobicity between aromatic and peptidic component can form (worm like) micellar structure with the aromatics still stacked, but the peptidic components thought to be disorganised.[245]

4.1.1 Parallel statcking of aromtic peptide amphiphiles

Parallel stacking (Fig. 17(a)) arrangements have been proposed for a variety of side chain halogenated Fmoc-F and Fmoc-Y derivatives (Fig. 18). This assignment is partly based upon CD signals at 270-310 nm and 200-230 nm, which are attributed to chiral Fmoc-Fmoc and phenyl-phenyl stacking interactions respectively.[132] Furthermore, XRD (X-ray diffraction) spacings of 14 and 30 Å are proposed to be consistent with the length of a single Fmoc-(penta-fluorinated)-phenylalanine molecule and the association of multiple parallel fibrils, respectively; such that the relatively hydrophobic Fmoc moiety remains buried in the core, whilst the carboxylates interact with the aqueous medium.[180] This proposed structure, based upon buried hydrophobic groups and parallel H-bonded stacking (4 Å XRD spacing) interactions, is analogous to the fibrous aggregation arrangements seen for longer, predominately aliphatic, peptide amphiphile systems.[293–297,102]

The pH dependence of the self-assembly process is also cited as an argument for the parallel stacking arrangements of these Fmoc-F and Fmoc-Y based systems,[109] since at high pH adjacent carboxylates would be expected to repel one another and preclude self-assembly and gelation. However, substantial apparent pK_a shifts are often observed for aromatic peptide amphiphile hydrogels in general (irrespective of the proposed stacking arrangement); with self-assembly occurring at a higher pH than would intuitively be expected,[171,210] (see Section 3.4) suggesting that, for these examples, carboxylic acids are in a hydrophobic environment.

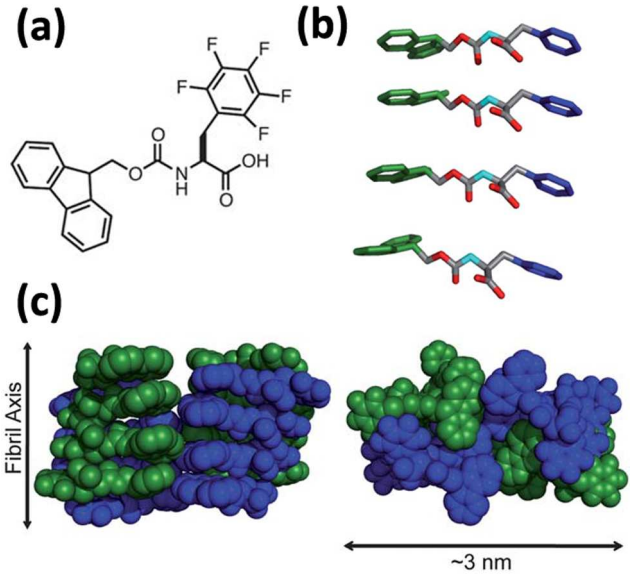

Figure 18 (a) Penta fluorinated Fmoc-F (a representative example of a Fmoc-F/Y derivative); (b) Parallel stacking arrangement; (c) Further aggregation of the elementary stacks. Adapted from Ref. [10] with permission from The Royal Society of Chemistry.

It could also be argued that single amino acid gelators such as these, are not necessarily representative of other aromatic (e.g. di- and tri-) peptide amphiphiles, since the single carbamate group precludes the formation of any β-sheet type H-bonding arrangement. For example, a separate study has shown that whilst a single amino acid gelator apparently lacks FTIR signals pertaining to a secondary H-bonding structure, equivalent dipeptide derivatives do show characteristic β-sheet and random coil type contributions around 1630 cm^{-1} and 1656 cm^{-1}, respectively.[241] Hence, this indicates a potentially distinct supramolecular arrangement associated with aromatic amino acid amphiphiles.

4.1.2 Antiparallel

Despite the proposed parallel stacking structure of discussed Fmoc-Phe derivatives (Fig. 18), an antiparallel arrangement (e.g. similar to Fig. 17 (b)) could also be energetically advantageous in some instances given the potentially complementary aromatic stacking interactions between Fmoc and, for example, the electron deficient penta-fluorinated phenylalanine ring system.[180] In any case, aromatic peptide amphiphiles that also possess aromatic side chains have the option of adopting an antiparallel conformation (Fig. 17 (b)). For instance, a naphthalene-FFGEY derivative is believed to adopt an antiparallel structure, with a β-sheet type H-bonding arrangement indicated by positive (near 196 nm) and negative (near 215 nm) CD bands.[45] The lack of significant excimer formation at 450 nm, and the presence of a shoulder above 400 nm adjacent to a monomeric naphthalene peak at ~340 nm by fluorescence, indicates naphthalene-phenyl

stacking interactions as opposed to extensive naphthalene-naphthalene stacking.

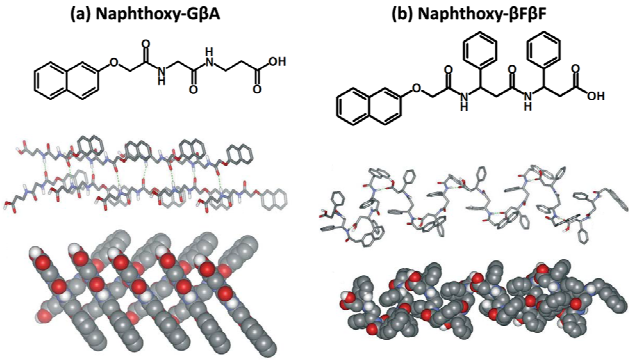

Figure 19 Aromatic side chains lead to an apparent disruption of parallel stacking arrangement. Adapted from Ref. [157] with permission from The Royal Society of Chemistry.

Aromatic residues are also shown to be a prerequisite for the antiparallel conformation in a study where distinct stacking arrangements have been proposed for aromatic peptide amphiphile with different dipeptide sequences.[157] With naphthoxy-GβA exhibiting stronger naphthalene stacking interactions than naphthoxy-βFβF on account of an increased fluorescence emission redshift. This is rationalised on the basis of naphthoxy-GβA adopting a parallel aromatic stacking arrangement, featuring H-bonding interactions with at least two other monomers, with layers almost perpendicularly orientated with respect to one another (Fig. 19 (a)). In comparison, naphthoxy-βFβF is proposed to assemble through H-bonding between the amide group adjacent to the naphthalene and the terminal carboxylic acid, thus giving rise to a helical structure (Fig. 19 (b)) that assembles into fibres through the further aggregation of these helices. Hence, it can be surmised that if there is aromaticity associated with the peptidic part of the gelator, then this can potentially compete with the nominal stacking of the N-terminal aromatic groups.

4.1.3 Interlocked antiparallel

As alluded to, a distinct antiparallel arrangement can be envisaged whereby stacks of H-bonded peptides are interlocked *via* antiparallel stacking between adjacent N-terminal groups (Fig. 17 (c)).[202,129,204,164,169,111] This interlocking mechanism addresses the disparity in aromatic stacking distances that would otherwise arise from this conformation – with aromatic groups on the periphery of a single H-bonded stack being spaced too far apart for effective overlap.[164] Henceforth, this will be referred to as the interlocked antiparallel stacking arrangement (Fig. 17 (c)), to avoid confusion with the aforementioned antiparallel structure (Fig. 17 (b)), which requires an aromatic amino acid side chain to satisfy head to tail stacking interactions.

4.1.4 Aromatic stacking conformations

The stacking conformation of the popular Fmoc moiety has been hypothesized to adopt a number of possible aromatic stacking conformations. These structural assignments have been made partly on account of the various fluorescence emission bands normally observed for these materials,[298,139] with gelation often accompanied by a redshift in the emission spectrum (Fig. 20).[245,235,22]

For instance, Fmoc-LG is proposed to exhibit an interlocked antiparallel stacking arrangement on the basis of a fluorescence emission redshift from 320 to 330 nm.[166] With self-assembly and gelation also accompanied by an increasing CD signal. Similar results are also observed in a study that included Fmoc-LL and Fmoc-LG hydrogels, with an emission redshift from 313 to 317-330 nm attributed to an interlocked antiparallel fluorenyl stacking arrangement.[289,163] Furthermore, a fluorescence shift from 309 to 323 associated with the co-assembly of Fmoc-L and Fmoc-K, is also thought to coincide with a predominately interlocked antiparallel arrangement in the gel state.[137] However, the existence of a shoulder at 380 nm is believed to be indicative of a portion of parallel Fmoc-Fmoc interactions – this is in agreement with the excimer emission observed for an intramolecular parallel fluorenyl interaction.[298] Closely related is the attribution of a similar shoulder at 370-380 nm to parallel interactions where micelles or micellar aggregates rather than fibres were observed.[258,289] Furthermore, parallel, antiparallel, and interlocked antiparallel dimers are suggested to be present for a Fmoc-Y system on the basis of 400, 350, and 380 nm peaks, respectively.[139]

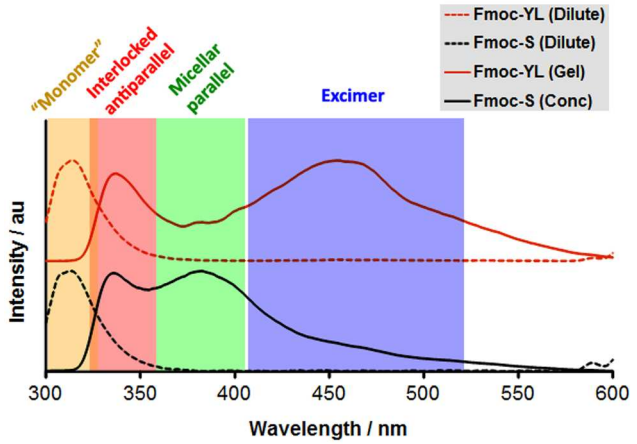

Figure 20 Typical fluorescence emission spectra for Fmoc peptide amphiphiles with some characteristic emission bands highlighted. Spectra adapted with permission from S. Fleming *et al.*, Biomacromolecules, 2014, **15**, 1171–1184.[245] Copyright 2014 American Chemical Society.

In addition, there is also often an excimer emission peak at approximately 450 nm from the extended aggregation of these aromatic moieties. Hence, there appears to be some inconsistency in the interpretation of these characteristic fluorescence bands, and the field would benefit from a comprehensive assessment of their supramolecular origins. However, generally speaking, a more pronounced redshift corresponds with a more extensive aromatic stacking arrangement. However, the variety of stacking conformations proposed also indicates that various stacking arrangements can potentially co-exist, depending upon any aromaticity associated with the peptide component, and the degree of disorder associated with a particular system.

4.1.5 H-bonding within the supramolecular stacks

In addition to the aforementioned aromatic interactions, H-bonding between peptide backbone residues is also likely to contribute to any proposed stacking conformation. Hence, FTIR absorptions at ~1685 and ~1625 cm^{-1} have been extensively utilised as experimental evidence of an antiparallel β-sheet type arrangement associated with aromatic peptide amphiphile based

hydrogels.[38,47,41,116] However, these characteristic assignments originate from the elucidation of secondary protein structures, where the higher wavenumber peak at ~1685 cm^{-1} is associated with an antiparallel structure.[299] Whereas, for aromatic peptide amphiphiles, the 1685 cm^{-1} band actually originates from the carbamate of the Fmoc functionality (Fig. 21).[116,208,245]

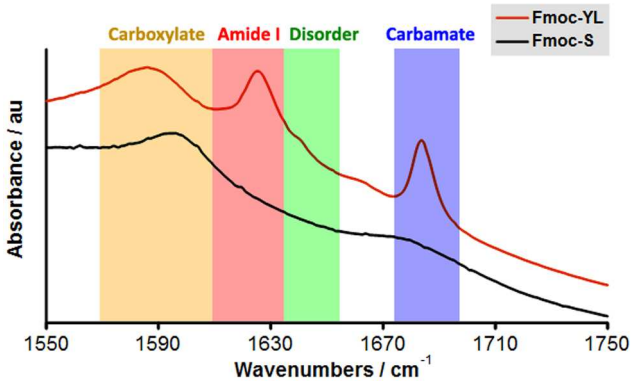

Figure 21 Typical FTIR spectra for Fmoc peptide amphiphiles with some characteristic absorption bands highlighted. Also illustrates a clear difference between H-bonding found in fibrous Fmoc-YL compared to Fmoc-S. Spectra adapted with permission from S. Fleming *et al.*, Biomacromolecules, 2014, **15**, 1171–1184.[245] Copyright 2014 American Chemical Society.

Nevertheless, FTIR amide I peaks can indicate the formation of an extended β-sheet type H-bonding structure, which in conjunction with other techniques may be interpreted as antiparallel. For instance, Fmoc-βAH is proposed to adopt an antiparallel, aromatic stacked, β-sheet type structure on the basis of characteristic amide I bands at 1636 and 1684 cm^{-1} by FTIR, and XRD spacings of 3.2 Å, 4.6 Å, and 12.4 Å providing evidence for aromatic stacking, β-sheet type H-bonding, and inter-sheet stacking distances, respectively.[86] Furthermore, the antiparallel arrangement is suggested for a variety of other aromatic peptide amphiphiles from FTIR, fluorescence, and XRD results.[33] Here, as discussed above, the fluorescence redshift is cited as evidence of an interlocked antiparallel fluorenyl conformation. In addition, the XRD spacings of 3.5 Å, 4.6 Å, and 9.4 Å are indicative of Fmoc-Fmoc stacking, inter-strand β-sheet type H-bonding, and inter-sheet stacking distances, respectively. This suggests an overall supramolecular conformation composed of antiparallel H-bonded stacks, which are then interlocked with aromatic stacking interactions (Fig. 17 (c)).[164,185]

Hence, besides the overall hydrophobicity, H-bonding interactions and by extension the peptide sequence also have important implications for the structural and physical properties of most aromatic peptide amphiphiles (as alluded to previously in Section 3.3.3).[154] For instance, when various glycine residue substitutions are applied to the popular Fmoc-FF and Fmoc-LL hydrogel systems, some trends are observed.[127,289] Although all sequences form supramolecular structures primarily through hydrophobic interactions. The Fmoc-GF and Fmoc-GL systems precipitated, whereas Fmoc-GG formed a meta-stable gel that precipitated over time. Only in the Fmoc-FG and Fmoc-LG examples (also see[166]) where the phenylalanine or leucine residue is adjacent to the N-terminal Fmoc moiety does stable gelation take place. Here, the position of the flexible glycine residue – that is not predisposed to form β-sheets – clearly influences whether or not the supramolecular stacking arrangement is conducive to gelation; with overly flexible examples exhibiting less propensity for forming a β-sheet type H-bonding arrangement as assessed by FTIR (~1685 and ~1625 cm^{-1}) and WAXS (wide angle X-ray scattering) (~4.6 Å inter-strand spacing). Hence, the order of the peptide sequence (Section 3.3) is again seen to have consequences for backbone flexibility and H-bonding conformations available to the molecule. Overall, as a rule of thumb for Fmoc dipeptides, a relatively flexible residue (e.g. glycine) in the first position increases the likelihood of precipitation as opposed to facilitating gelation – by disfavouring the formation of a β-sheet type H-bonding arrangement.

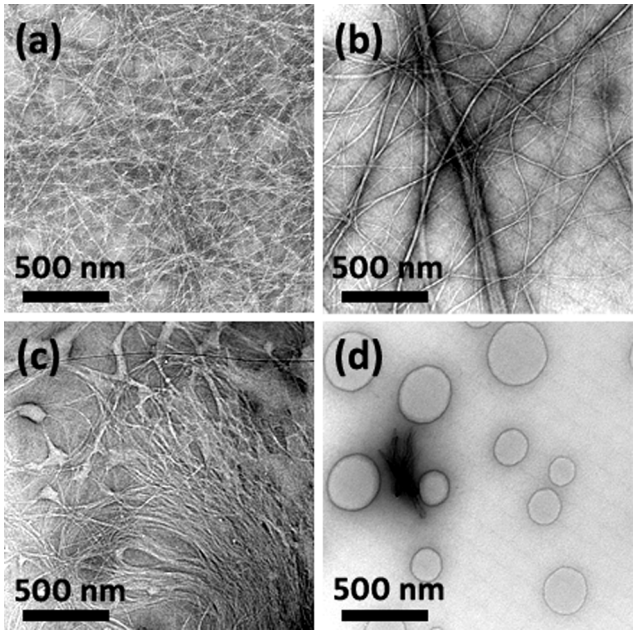

Figure 22 TEM images of (a) Fmoc-YS; (b) Fmoc-YT; (c) Fmoc-YN; and (d) Fmoc-YQ based nanostructures. Adapted from Refs. [204,220] with permission from The Royal Society of Chemistry.

Similarly, studies of Fmoc-YT, Fmoc-YS, Fmoc-YN, and Fmoc-YQ reveal apparent correlations between hydrogelation ability and the inference of a β-sheet type arrangement by FTIR.[220,204] Here, YS and YN exhibit amide I modes around 1640 and 1680 cm^{-1}, which are also accompanied by fibrous nanostructures (Fig. 22 (a, c)) and hydrogelation. Whereas in comparison, Fmoc-YT exhibits only the 1680 cm^{-1} FTIR contribution and forms a viscous nanofibrous (Fig. 22 (b)) solution – this result is interesting as the FTIR results indicate that only the carbamate is contributing to an internal H-bonding structure. In stark contrast, Fmoc-YQ demonstrates no apparent carbamate/amide internal H-bonding organisation and only spherical nanostructures (Fig. 22 (d)). Hence simple steric effects from additional methylene or methyl units can clearly have an influence on the available H-bonding arrangements and corresponding nanostructures.

4.1.6 Disorder in the supramolecular assembly

In addition to the proposed supramolecular models that feature a β-sheet type arrangement with ordered aromatic stacking interactions, disorder is likely to be a significant aspect of the supramolecular structure.[239] This is evidenced, by for example the

"random coil" type contributions (~1650 cm^{-1}) visible within the FTIR spectra of many gels,[289,116,129,19] with the relative intensity of this band seen to vary, thus indicating a varying degree of disorder and heterogeneity associated with these materials.

For example, from computational simulations and accompanying experimental data, a prominent "polyproline II" type conformation (i.e. a supramolecular structure lacking substantial internal H-bonding interactions) has been proposed for the Fmoc-AA system.[207,253] Computational simulations were initiated using starting structures based upon various parallel stacking conformations; with the aromatic groups concentrated at the core, whilst the peptides point out towards the aqueous interface.[180] These starting structures were found to be unstable, with a more disordered "polyproline II" type conformation observed after the simulations were completed. Furthermore, instead of a β-sheet type structure, results showed prominent H-bonding interactions with water and between the carbamate and terminal alanines. In addition, a closely related compound – Fmoc-A-lactic acid – which omits the amide bond of Fmoc-AA, also forms (weaker) hydrogels, indicating that this H-bond donor is not required for gelation.[253] Torsion angles[130,173] also inferred an apparent preference for "polyproline II" conformations; although some angles characteristic of antiparallel structures were also observed. Experimentally, WAXS demonstrates the presence of a 4.35 Å spacing, which on account of computational results was assigned to aromatic stacking as opposed to β-sheets. The authors also report some FTIR and CD absorptions typically attributed to β-sheet type structures. However, the authors note that the CD peak positions are shifted with respect to proteins, and the FTIR also shows a prominent absorption at 1644 cm^{-1}, which is assigned to random coil type structures. In terms of a higher order assembly mechanism, the authors note that the supramolecular "polyproline II" type structure yields an amphiphilic surface, with some of the Fmoc moieties exposed to the bulk. These hydrophobic features on the surface of the elementary fibres may help to facilitate further aggregation mechanisms between fibres, resulting in extensive interconnectivity.

Similarly, Fmoc-AA and Fmc-AA experimental and computational FTIR results were the subject of a recent study from our group.[116] Here, simulated FTIR spectra from parallel and antiparallel supramolecular H-bonding arrangements demonstrated that the 1685 cm^{-1} peak is indicative of the carbamate functionality, and not of a specific intermolecular H-bonding arrangement. In addition, while on this basis it was not possible to unambiguously assign a parallel or antiparallel structure, the experimental FTIR spectra do correlate more closely with the simulated antiparallel spectra.

Overall, these are both illuminating studies on Fmoc-AA – the simplest aromatic dipeptide amphiphile with chiral amino acids – highlighting that disorder is likely to be a significant factor in the supramolecular assembly of aromatic peptide amphiphile materials, and that protein secondary structure analogies should be applied with a degree of caution. However, given the limited simulation sizes, edge effects are likely to disproportionately affect the computational results. Hence, using computational approaches to help elucidate supramolecular structures remains a challenge but is expected to become more important as computational power and simulation methodologies improve.

4.1.7 Worm like micelles

It is possible for aromatic peptide amphiphiles to form worm like micelle structures if there is a more significant amphiphilic imbalance between the aromatic and peptide component. For example, for aromatic peptide amphiphiles not predisposed to form a β-sheet type H-bonding arrangement, worm like micelles can be the preferred arrangement even at lower pH values (e.g. 6.5).[245] Pyr-S has been found to form a hydrogel consisting of worm like micellar structures on the basis of the directionality associated with the aromatic stacking of planar pyrene moieties. In this system, the enhancement of the carbonyl vibrations typically seen by FTIR for similar supramolecular materials is not observed.

The amphiphilicity of aromatic peptide amphiphiles is also sensitive to environmental factors, such as pH. For instance, one fairly intuitive proposal is the adoption of worm like micelle structures at high pH, with the charged carboxylates at the surface and the aromatic moiety buried in the core.[190] The presence of worm like micelles has been inferred by sample viscosity and *via* the observation of structures by TEM at high pH. Here, crosslinking of the surface carboxylates could also be facilitated using divalent cations to improve the network integrity. Supporting the cation crosslinking worm-like micelle model is the observation that the gelation of various naphthoxy-dipeptide derivatives at high pH is most easily facilitated by divalent cations such as Mg and Ca, as opposed to monovalent Li, Na, or K.[190] Hence, crosslinking interactions between worm like micelles allow for aromatic peptide amphiphiles to undergo hydrogelation over a wider pH range, altering the morphology and properties of the fibrous network in the process.

Since TEM fibrils and fluorescence emission peaks at ~375 nm corresponding to micellar aggregates have been reported for Fmoc systems at high pH,[289,127] and a preference for parallel stacking interactions between Fmoc moieties have been inferred by molecular dynamics simulations at relatively low (virtual) subgelation concentrations,[233] we believe that micellar aggregation is a more general phenomena associated with aromatic peptide amphiphiles while in the relatively ionised state – the addition of divalent cations simply allows for gelation to take place under these conditions.

Hence, worm like micelle systems are inherently more disorganised, since these structures lack the ordered H-bonding arrangements normally associated with peptide amphiphiles.[289,127] This distinct supramolecular structure associated with aromatic peptide amphiphiles, simply represents a different, more disordered aggregation process. Either before the pH is lowered and extended H-bonding begins to lock the network into place,[171] or because the system simply lacks the ability to form an ordered H-bonding arrangement irrespective of pH.

4.2 1D and 2D growth mechanisms

Beyond the discussed stacking conformations (Fig. 17), evidently, further aggregation mechanisms are responsible for the 1D fibrous morphologies normally observed in the resulting nanostructured materials. In this subsection two main, potentially competing, growth mechanisms are proposed.

4.2.1 Coiling tape mechanism

Curvature associated with the (e.g. interlocked) H-bonded

stacking structure is ultimately responsible for the observed supramolecular chirality,[115] this is important, because in general self-assembly terms, chirality has been cited as a key factor or requirement for self-assembly into fibres/nanotubes.[300–302] Here, for what shall be referred to as the coiling tape mechanism (Fig. 23), elementary tapes, which would otherwise form 2D structures via lateral growth, develop into twisted and then coiled tapes over the course of the self-assembly process.[121] This closing mechanism is found to proceed *via* a combination of two possible routes; growing width and closing pitch (increasing helicity) of the elementary tape. Finally when the coiled tapes close over, the resultant fibre or nanotube morphology is obtained. For aromatic peptide amphiphiles, the outside and/or core of this structure could potentially be stabilised *via* hydrophilic and/or hydrophobic amino acid side chains respectively.

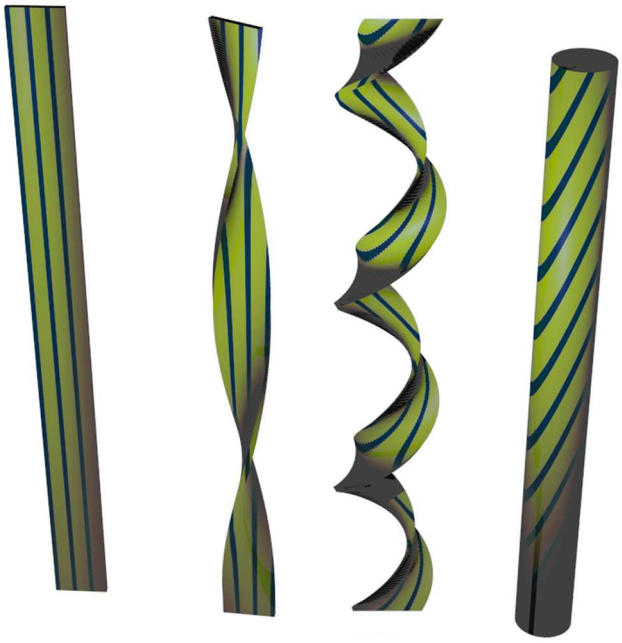

Figure 23 Depicts coiling tape mechanism (as applied to aromatic peptide amphiphiles featuring interlocked antiparallel stacking conformation – with aromatic and peptide stacking shown in blue and yellow respectively).

For example, the ubiquitous Fmoc-FF system (Fig. 24) has been proposed to give an interlocked antiparallel stacking conformation, followed by a higher ordered aggregation mechanism that in part appears to be akin to the coiling tape growth mechanism (Fig. 23).[164] Similar to previous examples the intermolecular stacking arrangement is supported by ordered H-bonding interactions by FTIR, and a 218 nm peak by CD that is also attributed to this β-sheet type arrangement. In addition, the interlocking of these β-sheet stacks is inferred from a fluorescence shift to 330 nm suggestive of an antiparallel orientation of the Fmoc groups.[137] Furthermore, this system exhibits a fluorescence excimer at 460 nm, indicating extensive J-aggregate formation. Due to a twist present in the β-sheet which is a consequence of the presence of chiral centres,[303] the sheets are believed to rotate to allow full fluorenyl overlap. Overall this results in a cylindrical arrangement, with four interlocked sheets forming a the pseudo-tertiary structure 30 Å in width, with a 7 Å cavity in the centre. Further side by side aggregation of these cylindrical structures, yields the observed ribbons by TEM (transmission electron microscopy). These proposals are also supported by WAXS, which features several of the spacing that would be characteristic of this supramolecular assembly. Nanotubes are also observed for the Fmoc-LLL system, with several β-sheets interlocked *via* aromatic stacking.[185] In this case multiple (e.g. three) β-sheet layers are proposed to be associated with a given cylinder – as indicated by WAXS and illustrated by molecular dynamics simulations. Overall, for both Fmoc-FF and Fmoc-LLL, the curvature associated with the interlocked sheets provides the basis of 1D fibrous/cylindrical assembly, *via* the coiling tape mechanism, as opposed to an infinite 2D sheet.

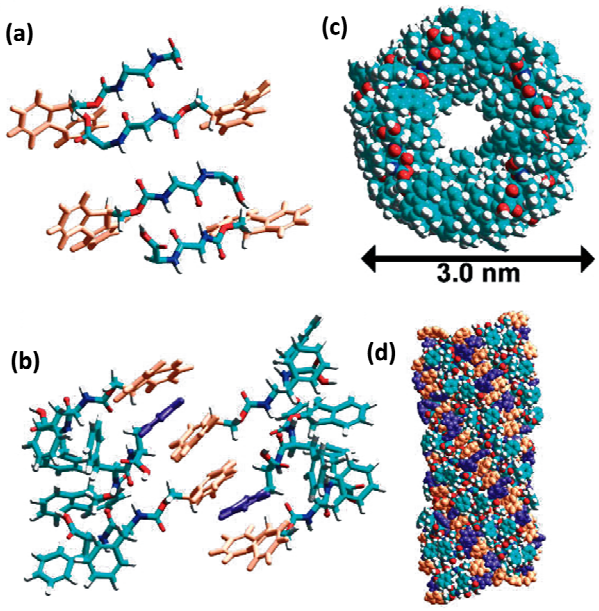

Figure 24 Supramolecular structure of Fmoc-FF; (a) interlocked antiparallel arrangement, (b) sheet helicity, (c, d) cylindrical structure. Reproduced from Ref. [164] with permission from John Wiley and Sons.

4.2.2 Helical lamellar growth mechanism

A similar fibrous aggregation mechanism is also proposed on the basis of helicity.[303] Here, with increasing concentration, helical tapes undergo plane-to-plane bilayer and then lamellar type stacking interactions to form ribbons, fibrils, and finally fibres. Hence, the lateral growth of the elementary tapes is inherently limited by their helicity, explaining why 2D structures are not generally observed. In addition, an infinite lamellar stack composed of these tapes is also generally disfavoured on the basis of helicity. Hence, this shall be referred to herein as the helical lamellar growth mechanism (Fig. 25 (a-c)), where for the specific case of aromatic peptide amphiphiles, lamellar type stacking would be stabilised *via* complementary peptide side chain interactions (Fig. 25 (d)).

For example, systems proposed to adhere to the helical lamellar model have been found to be sensitive to small changes in the peptide sequence, with the sterics associated with peptide side chains a major factor, as has been observed for a range of Fmoc dipeptide methyl ester systems.[129] Here, as alluded to previously (Section 4.1.3), spectroscopic evidence suggests that the underlying aromatic stacking (e.g. by fluorescence redshift

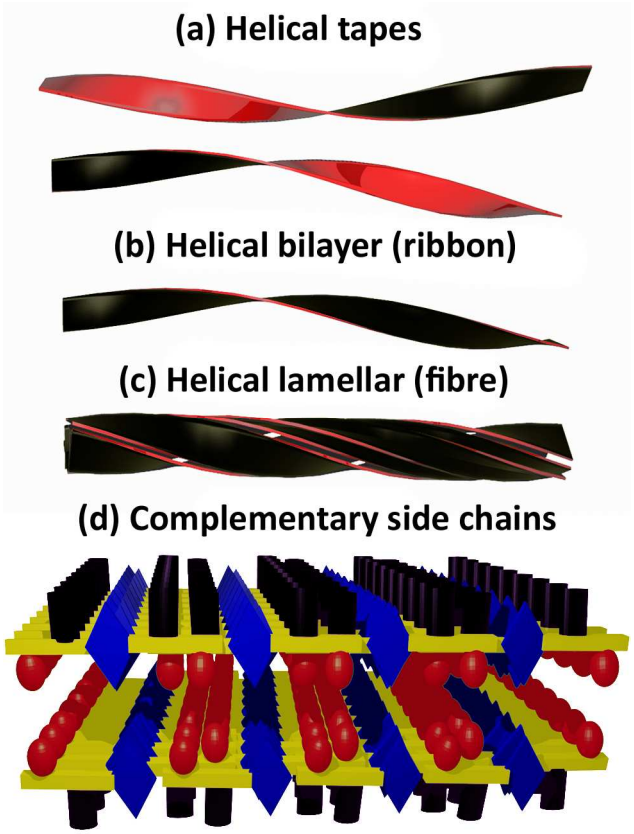

Figure 25 Depicts helical lamellar growth mechanism, where red and yellow faces refer to generic self-complementary interactions: (a) helical tapes; (b) helical bilayer (ribbon); (c) helical lamellar (fibre); and (d) a more detailed illustration of self-complementary side chain interactions.

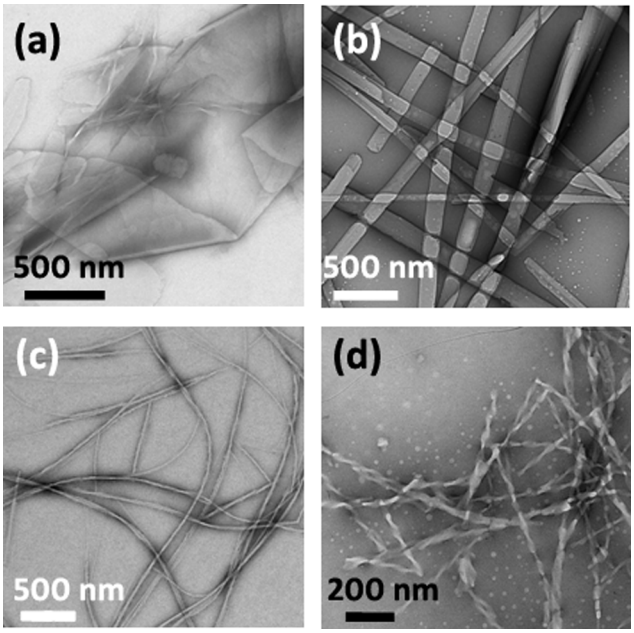

Figure 26 TEM images of (a) Fmoc-SF-OMe, (b) Fmoc-SL-OMe, (c) Fmoc-TF-OMe, and (d) Fmoc-TL-OMe based nanostructures. Adapted from Ref. [129] with permission from The Royal Society of Chemistry.

and excimer formation) and H-bonding (by FTIR) processes underpinning the interlocked antiparallel assembly process are similar across the systems; Fmoc-SF-OMe, Fmoc-TF-OMe, Fmoc-SL-OMe, and Fmoc-TL-OMe. In addition, similar characteristic spacings are observed by WAXS; 3.8 Å Fmoc stacking, 4.6 Å β-sheet type H-bonding, and a ~15 Å spacing from the length of the peptide backbone. Despite this, different supramolecular architectures are seen to be dependant upon minimal changes to the peptide sequence. For instance, a hydrophilic serine residue adjacent to the Fmoc moiety (Fig. 26) induces more planar structures, with Fmoc-SF-OMe being the most dramatic example – exhibiting 2D sheets.[110] In contrast, when serine is substituted for threonine, this promotes the formation of 1D fibres or twisted ribbons. These dramatic morphological differences can be explained on the basis of minimising water contact with the additional methyl group of threonine, thus inducing a twist in the supramolecular structure. Furthermore, the additional chiral centre associated with threonine may also be an important factor in promoting chiral assembly. In any case, Fmoc-SF-OMe is believed to promote a planar structure *via* the formation of a bilayer exhibiting an extensive lateral growth mechanism (e.g. Fig. 25 (d)); with the hydrophobic phenylalanine residues buried within the structure, whilst the hydrophilic serine residues interact with the aqueous phase. These planar structures associated with SF and SL are also supported by a WAXS spacing of ~9.3 Å, which could coincide with the side chain spacings between interacting sheets. It is also possible that these bilayers could assemble further in a lamellar fashion. TEM results suggest a possible mechanism for sheet formation; initially twisted ribbons are observed to undergo branching, while later the nucleation of ribbons can be observed from the edges of the nanosheets. These apparent intermediary structures indicates that there is a fine balance between the 2D nanostructures observed for this system, and the 1D fibres normally obtained. This is partly ascribed to the enzymatic amide condensation assembly mechanism used in this instance – a reversible process driven by the attainment of the most thermodynamically favourable nanostructures.

In an example that is similar to the hydrophilic/-phobic sequence of Fmoc-SF-OMe, the aggregation of aromatic interlocked antiparallel β-sheets type structures may also be subject to the lamellar growth mechanism. For instance, the Fmoc-KK(NDI) system is proposed to form "nanobelts" (i.e. bilayer tape structures with limited lateral growth), where the Fmoc interlocked sheets assemble in a face to face manner that utilises the aromatic stacking of the n-type NDI groups, whilst the unfunctionalised lysine residues point outwards into the aqueous medium (e.g. Fig. 25 (b, d)).[111] Here, stacked K(NDI) side chains and separately stacked N-terminal Fmoc groups stabilise the H-bonded antiparallel dilysine supramolecular arrangement. This material exhibits substantial fluorescence quenching upon self-assembly, and is potentially well suited for 1D charge migration. The supramolecular arrangement is supported by characteristic XRD spacings, and fluorescence emission spectroscopy which suggests orthogonal Fmoc-Fmoc and NDI-NDI aromatic stacks. However the mechanism responsible for inhibiting the continued lateral assembly of the Fmoc interlocked structures is unclear. It is possibly the charge associated with the lysine residues that limits the aggregation mechanism, as if there is a helicity associated with the ribbons then lateral growth would bring these surface charges into close contact with one another. Alternatively,

continued lateral growth may be kinetically disfavoured. In addition, the fact that the previously described sheets of Fmoc-SF-OMe were assembled under thermodynamic control,[110] suggests that elementary stacking imperfections may contribute to the inherent helicity of the interlocked β-sheet type structures.

Elsewhere, a study of various Fmoc-peptide (e.g. FF, FRGD, RGDF) gelators has found XRD spacings of about 4.7 Å and 10 Å, associated with the β-sheet interstrand stacking and lamellar stacking distances, respectively.[113] Here, it was observed that the latter stacking distance was variable depending upon the precise peptide sequence employed. Hence, while the precise mechanism and supramolecular structure may be dependant upon the peptide sequence or gelation protocol utilised, it is clear that supramolecular chirality is important for the formation of 1D nanostructures.

4.2.3 Gelation versus crystallisation

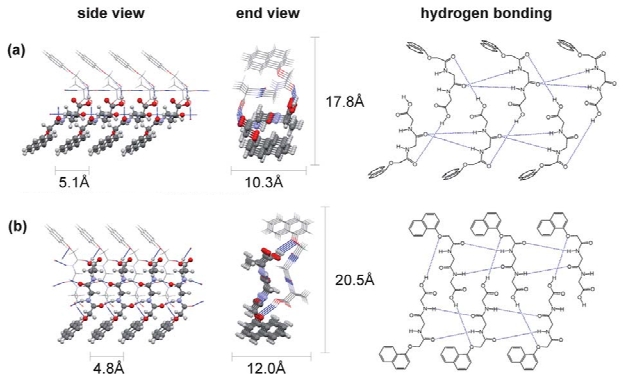

Figure 27 An example of a 1D compact stacking arrangement predicted for naphthoxy-GA. Adapted from Ref. [173] with permission from The Royal Society of Chemistry.

Hence, despite the predominance of 1D aromatic peptide amphiphile nanostructures, 2D structures can also be obtained depending upon the peptide sequence. In this respect, efforts have been made to rationalise similar behavioural differences between a naphthoxy-GA meta-stable hydrogel and a naphthoxy-AG crystalline material.[173] Computed packing arrangements and XRD experiments suggest that 1D H-bonded molecular aggregates are energetically more favourable for the successful gelator, whereas the crystalline material preferentially exhibits a 2D H-bonding network. Both systems demonstrate potential 1D stacking arrangements composed of "open tapes", which possess a parallel conformation with aromatic stacking at the periphery, and carboxylic acids H-bonding with one another at the centre between two parallel molecular stacks. However, only the naphthoxy-GA hydrogelator exhibits a significant number of relatively low energy, "compact", 1D H-bonding arrangements. These stacking arrangements, similarly feature parallel H-bonding and aromatic stacking interactions, but often with the carboxylic acids H-bonding to an amide carbonyl or the naphthoxy oxygen (Fig. 27). The angle between the aromatic and peptide is also suggested as a reason for the differential self-assembly behaviour of these systems. This is a concept that was previously discussed in section 3.2, whereby naphthoxy linkers displayed the greatest potential for hydrogelation on the basis of a relatively linear molecular conformation.[130] These findings reinforce the complexities associated with supramolecular self-assembly, and reiterate the multitude of proposed stacking arrangements. However, a similar theme re-emerges; the fine balance between 2D crystallisation/precipitation and 1D fibrous hydrogel assembly may result from small changes in molecular structure.

5. Co-assembly of aromatic peptide amphiphiles

Finally, the co-assembly of different aromatic peptide amphiphiles can be a useful means of modifying the properties of the resultant materials in a modular fashion.[22,23,40,258]

5.1 Co-assembly: the relative affinity of individual constituents

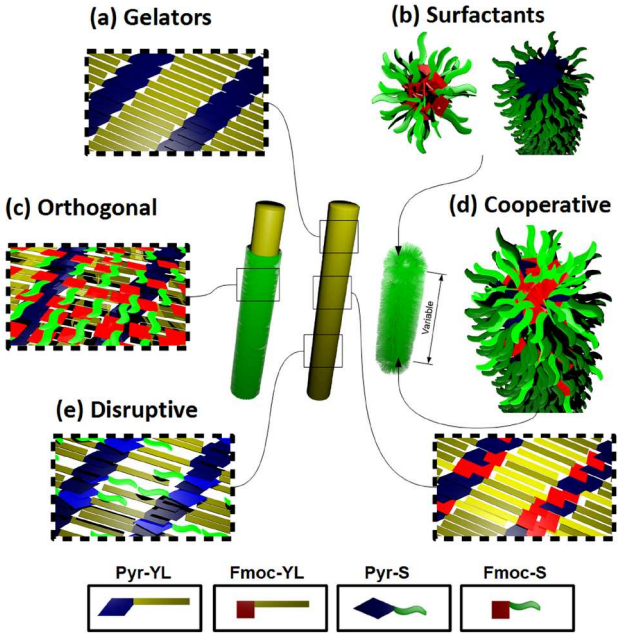

Figure 28 Co-assembly architectures are influenced by both the aromatic and peptide parts of corresponding co-assembly constituents. Adapted with permission from S. Fleming *et al.*, Biomacromolecules, 2014, **15**, 1171–1184.[245] Copyright 2014 American Chemical Society.

The degree of nanoscale phase separation observed between aromatic peptide amphiphile co-assembly constituents has been shown to be influenced by the corresponding aromatic and peptide parts (Fig. 28).[245] For example, when Pyr-YL, Fmoc-YL, Pyr-S, and Fmoc-S are co-assembled in all possible 1:1 configurations, several trends bcome apparent. When constituents possess the same peptide component and differing aromatic segments, a mixed or so-called cooperative arrangement is formed, where either mixed interlocked antiparallel fibres (Pyr-YL/Fmoc-YL) or mixed worm like micelles (Pyr-S/Fmoc-S) are formed. In comparison when constituents possess the same aromatic moieties and differing peptide sequences. A so-called disruptive co-assembly is formed, whereby extensive aromatic stacking and intercalation of constituents takes place, which ultimately comprimises the H-bonding arrangement associated with the YL system, as observed by increased FTIR inhomogeniety and a decrease in CD signal intensity. Finally when constituents possess differing peptide and aromatic segments, the relatively hydrophilic serine constituent is found to coat the YL fibres without significant incorporation into the

underlying structure. These surfactant coated or so-called orthogonal systems generally exhibit spectroscopic and material properties indicative of their underlying YL fibres, with the serine surfactant only affecting the surface functionality. This fibre coating approach is of particular relevance for cell culture applications.[43,258,23]

5.2 Co-assembly: hydrophobicity, charge and chirality

Given that the self-assembly and gelation properties of aromatic peptide amphiphiles are strongly influenced by the overall hydrophobicity of the peptide sequence, it makes sense to further tune this attribute *via* co-assembly. This methodology assumes that co-assembly components yield a mixed supramolecular structure, featuring the usual aromatic stacking and H-bonding interactions between the constituents.[139,137] For example, a 1:1 ratio of Fmoc-FF and Fmoc-GG produces hydrogels with higher elastic moduli than Fmoc-FF alone.[192] This is despite Fmoc-GG failing to gel individually under similar conditions. In this instance, the optimal 1:1 ratio suggests that regular (possibly alternating) intercalation of Fmoc-GG into the Fmoc-FF fibres provides an effective balance for gelation. In comparison, Fmoc-FF/Fmoc-RGD hydrogels show the largest elastic moduli using 20% Fmoc-RGD content.[42] Similarly, this is indicative of Fmoc-RGD becoming an integral part of the Fmoc-FF fibrous structure. The co-assembly of Fmoc-FF, with Fmoc-K, Fmoc-S, or Fmoc-D similarly resulted in significant changes to rheological properties and fibre morphology.[43] Though it should also be noted that the rheological properties of the Fmoc-FF system are generally very sensitive to the preparative conditions employed.[210] Nevertheless, these results indicate that tailoring the hydrophobicity of Fmoc-FF fibres is a useful strategy for augmenting the hydrogelation properties of the system.

In other co-assembly examples, gelators can be chosen that have complementary characteristics. For example, when penta-fluorinated or mono-halogenated Fmoc-F derivatives are co-assembled with unfunctionalised Fmoc-F, this process is assisted by complementary interactions between the phenyl side chains, which possess differing electronic properties.[198] Given that penta- and mono- substituted derivatives gave similar enhancements in rheological properties; this is not believed to be mediated by face-to-face stacking of the phenyl groups, instead electronic effects from the halogen substituent(s) are believed to result in more subtle offset π-π interactions.

Similarly, electrostatics also have a role to play in the co-assembly of aromatic peptide amphiphiles, with oppositely charged Fmoc penta and hexa peptides co-assembling in this manner.[186] Individually, positively (Fmoc-KKRGDK) or negatively charged (Fmoc-VRGDV, Fmoc-GRGDG) peptides could assemble, but only in the co-assembly setup, where the charge is balanced, could gelation be effected at a neutral pH.

Co-assembly components can also be entirely interdependent upon one another for gelation. For example, the assembly of K or R with Fmoc-E, relies on complementary electrostatic interactions between the constituents – with the system effectively composed of a pseudo Fmoc dipeptide *via* an ionic as opposed to an amide bond.[189] In addition, in the same study, the chirality of the nanofibres was shown to be altered with different L-/D- compositions – where molecular chirality relates directly with supramolecular chirality. Here, racemic mixtures are also found to form hydrogels, but with a diminished CD signal and evidence of self sorting behaviour – or orthogonal assembly. Similarly for other systems, substituting D-alanine for L-alanine has a direct impact upon the observed supramolecular helicity,[36] with racemic mixtures exhibiting weaker rheological properties or precipitating.[130] This highlights the importance of chirality in the gelation process, and also demonstrates some of the challenges in predicting the co-assembly behaviour that will be observed.

5.3 Co-assembly: C-termini heterogeneity

A synergistic relationship between co-assembling aromatic peptide amphiphiles is a recurring theme in the literature with multicomponent gels often displaying robust mechanical properties, this same principle can also be applied to C-termini modifications.

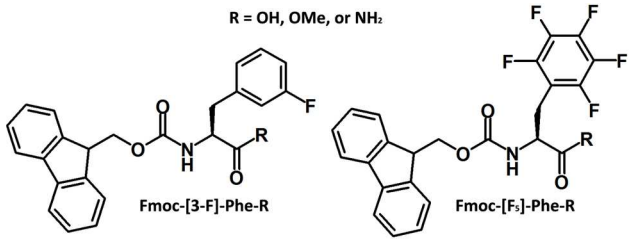

Figure 29 Structures of gelators used in C-termini co-assembly study.[109]

For instance, it has been shown that the co-assembly of penta-fluorinated Fmoc-F and its OEG functionalised C-termini equivalent, resulted in hydrogels with high elastic moduli and the ability to recover their mechanical properties.[181] In contrast, under the conditions used in this study, penta-fluorinated Fmoc-F itself only recovered 66% of its mechanical properties following the application of 100% strain, whilst the OEG analogue by itself exhibits 100% recovery but only weak gels in the first instance. Furthermore, although OEG based fibres were observed by TEM, no evidence of the pronounced helicity normally associated with these materials was inferred by CD – indicating that the OEG chains interfere with the parallel stacking conformation proposed for these systems. Upon co-assembly, the mechanical improvements were rationalised on the basis that heterogeneity helps to slow the precipitation of the penta-fluorinated Fmoc-F, which itself contributes rigidity to the co-assembly construct. In addition, the multicomponent material exhibits changes to the intensity and handedness of its CD spectrum depending upon the precise ratio used; indicating the formation of mixed fibres as opposed to self-sorting behaviour.

In another example, the co-assembly of side-chain halogenated Fmoc-phenylalanine derivatives with different C-termini was found to be useful for augmenting their respective self-assembly properties (Fig. 29).[109] The phenylalanine residue is too hydrophobic to undergo hydrogelation when used in conjunction with the COOMe functionality. Whereas, the corresponding amide derivatives generally give rise to solutions, being too hydrophilic to allow for effective gelation. Despite this, fibrils can still be observed by TEM in each case – indicating that co-assembly with the corresponding COOH variants may allow for the tuning of these hydrophobicities. COOH derivatives themselves form hydrogels at low pH, whereas in PBS solution

electrostatic repulsion of carboxylate anions compromises the mechanical properties of the hydrogel network yielding solutions. In this regard, the co-assembly of COOH and $CONH_2$ was generally found to be beneficial at high pH in PBS buffer – yielding hydrogels in each case. Hence, in this example, a non-gelating species assisted the gelation of a related molecule by helping to mitigate the effects of electrostatic repulsion; highlighting the utility of C-termini modifications within the context of co-assembly.

5.4 Co-assembly: self-sorting under pH control

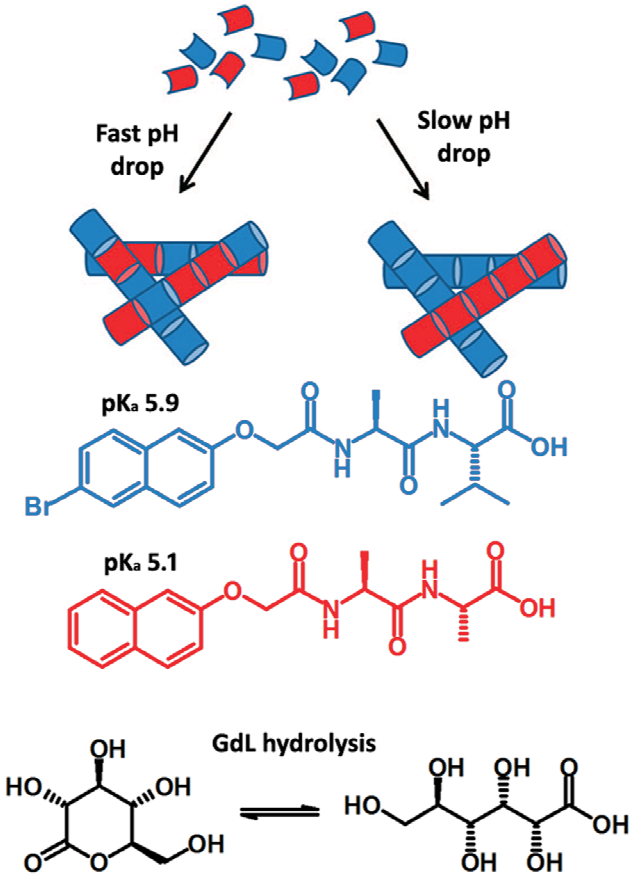

Figure 30 Self-sorting mechanism based on differential pK_a and corresponding gelation pH values. Slow pH drop is mediated *via* GdL hydrolysis. Adapted by permission from Macmillan Publishers Ltd: Nat. Commun. (Ref. [217]), copyright (2013).

In some instances, it is possible to control the co-assembly arrangement through a judicious choice of initiation methodology, which differentially controls the assembly kinetics for different components in a mixture. For example, if the maximum gelation pH or apparent pK_a values of the co-assembly constituents are different, then it is possible to control the co-assembly arrangement through pH control (Fig. 30).[217,246] In this instance, if the pH is altered slowly – by for example utilising GdL (glucono delta lactone) or alternatively the electrochemical decomposition of hydroquinone – then the higher pK_a gelator will begin to assemble first, as inferred by the NMR (nuclear magnetic resonance) silence of this species in the supramolecular state. As the pH continues to decrease the second gelator can then assemble independently of the first, resulting in an interpenetrating network. Alternatively if the pH is lowered rapidly, then there will be insufficient opportunity for self sorting behaviour, and instead the mixed kinetic product will be attained. Hence, this illustrates that the kinetics of the initiation method can also influence the co-assembly process – potentially resulting in orthogonal assembly.

6. Other factors affecting the self-assembly process

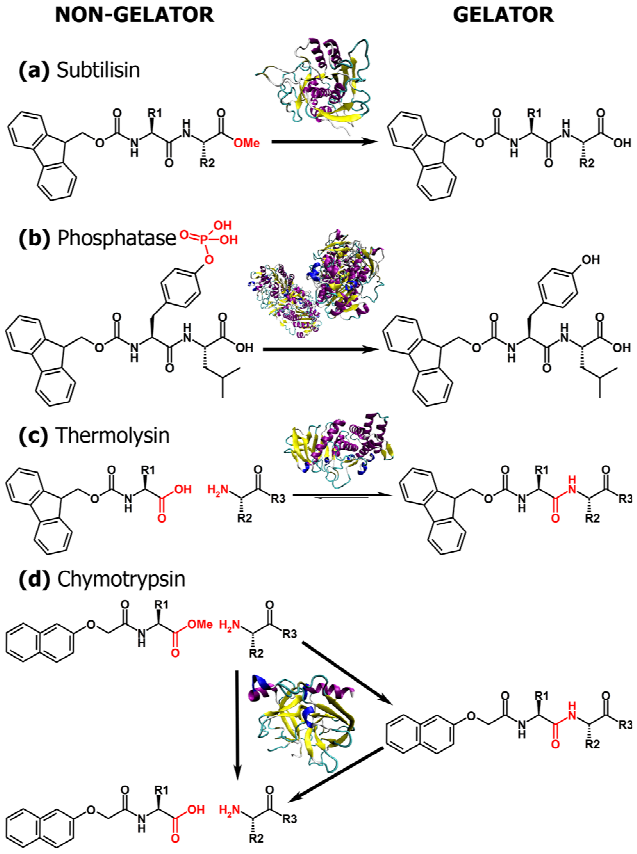

Figure 31 Summary of reported enzyme responsive hydrogelation examples including: (a) subtilisin methyl ester cleavage;[114,185,204,212] (b) phosphatase phosphate cleavage;[126,139,155,45,44,34,170,304,237,238,244,252] (c) thermolysin amide bond condensation;[3,110,129,158,163,167,184,218,250] and (d) chymotrypsin non-equilibrium (temporary) assembly.[231]

As is clear from the above, self-assembly is an extremely versatile but complicated process, driven by various intermolecular interactions that are inherently dependant upon the molecular structure of the gelator in question as well as the environmental conditions. However, another important aspect that can be considered is the means by which self-assembly is effected or augmented, i.e. kinetic aspects.[284,135] Ultimately, many hydrogels are thought to be in a kinetically-trapped, meta-stable state (akin to polymorphism as seen in crystallisation). Hence, a single gelator can potentially access a variety of supramolecular structures depending upon the self-assembly protocol (conditions, kinetics) utilised. In reality this relates to the formation of highly diverse materials from identical building blocks. For instance, seemingly simple parameters, such as variations in gelator concentration and temperature, will ultimately affect the apparent pK_a and the relative strength of the intermolecular interactions, thus impacting the self-assembly and gelation

process.[27,28,36,37,114,127,134,157,171,181,187,195,212,289,305] In addition, ions can also radically alter the hydrogel properties and the precise supramolecular arrangement adopted; *via* charge screening;[196] divalent cationic fibre crosslinking;[46,43,86,155,189,210,190] and kosmotropic/chaotropic considerations.[306,211,212]

Furthermore, traditional laboratory based hydrogel preparation methods usually involve altering the prevailing conditions such as pH, solvent composition and temperature. Hence, it is also important to consider the kinetics of the self-assembly process, and by extension the means through which self-assembly is initiated. For example, the adjustment of pH is a complex balance between encouraging the thermodynamically favoured aggregation of the gelator below its pK_a, and kinetic/heterogeneity considerations.[166,192] Using dropwise HCl addition to initiate assembly is difficult to control and reliably reproduce,[115,46,127,134,157,164,192,199] in contrast to the slow or controlled alteration of the pH that can be achieved by for example GdL decomposition,[112,128,131,166,172,173,176,210,255] or *via* electrochemical methods.[246,178,197] Similarly, gel preparation *via* the aqueous dilution of a concentrated DMSO, methanol, or hexafluoropropanol hydrogelator solution,[19,37,132,133,174,181,188,191,210,248,18] may be diffusion controlled – resulting in an uneven gelator distribution depending upon the kinetics of the hydrogelation process.

There is also increasing interest in using biocatalytic, enzyme catalysed reactions to control and direct molecular self-assembly.[4,45,160,307–309] This approach is inspired by biological systems, where assembly and disassembly of dynamic fibres is controlled by biocatalysis. Enzymatic processes utilise an inactive gelation precursor, which can be converted to the relevant self-assembling monomer in a controlled fashion and under constant conditions, usually by removal of a steric or electrostatic blocking group (see Fig. 31 for examples).[31,30,34,44,45,114,126,139,155,168,170,183,185,204,212,258,304] Hydrogel assembly using enzymes offers potentially unparalleled kinetic control, with the number of fibrous nucleation sites dictated by the concentration of enzyme. Furthermore, the reversed hydrolysis mechanism, mediated by proteases, such as thermolysin,[3,110,129,158,163,167,184,218] allows for self correction during the self-assembly process, as the system equilibrates towards a more thermodynamically stable state.[243] In addition, enzyme mediated non-equilibrium hydrogel systems have also been recently reported.[231]

Hence, by altering the route of self-assembly, the precise properties of the resultant materials can be changed, even if the underlying chemical compositions are identical. Although not fully addressed in this review, it is important to acknowledge that the gelation initiation methodology, can have a profound impact upon the thermodynamic and kinetic aspects that affect these inherently tuneable and dynamic aromatic peptide amphiphile based materials.

7. Conclusions

The self-assembly of aromatic peptide amphiphiles is based on a complex interplay of molecular, environmental, and kinetic considerations. Aromatic and peptidic functionality act in a synergistic fashion; contributing aromatic stacking and H-bonding interactions towards the self-assembly motif. Self-assembly and hydrogelation requires a balance of molecular characteristics; such as hydrophobicity, amphiphilicity, sterics, electronics, and a linear molecular geometry. In terms of the supramolecular structures associated with aromatic peptide amphiphiles; a variety of parallel, antiparallel, interlocked antiparallel, and more disordered stacking arrangements have been proposed. The adoption of a particular intermolecular stacking arrangement may depend upon a variety of factors, encompassing both the hydrogelator in question, the prevailing environmental conditions, and the degree of disorder and heterogeneity associated with the gelation methodology. Although the underlying assembly mechanisms may be similar, the emergence of a particular supramolecular structure is highly dependent upon subtle molecular alterations. For example, fibres, sheets, tubes, and spirals can be observed depending upon the sequence employed. Furthermore, a variety of higher order aggregation mechanisms have been proposed; including coiling tape and helical lamellar growth mechanisms, where the adoption of a 1D fibrous structure can be broadly explained on the basis of chirality and sterics, which normally act to disfavour extended 2D structures. Although other factors can also have a profound impact upon gel state materials, such as environmental and kinetic/heterogeneity considerations – these are largely outside the scope of this review. Nonetheless, through an appreciation of the subtle molecular, and supramolecular factors, aromatic peptide amphiphiles can begin to be tailored for given applications in a rational and systematic fashion. While the elucidation of many of these design rules is still in its infancy, aromatic peptide amphiphile systems clearly have great potential for the preparation of minimalist, dynamic, and biocompatible materials.

8. Acknowledgements

The research leading to these results has received funding from the European Research Council under the European Union's Seventh Framework Programme (FP7/2007-2013) / ERC grant agreement n° [258775].

9. Notes and references

[a] *WestCHEM/Department of Pure and Applied Chemistry, Thomas Graham Building, 295 Cathedral Street, University of Strathclyde, Glasgow G1 1XL, United Kingdom. E-mail: scott.fleming@strath.ac.uk*
[b] *Advanced Science Research Center (ASRC), City University of New York, New York, NY1003, USA E-mail:Rein.Ulijn@asrc.cuny.edu*

1. J. F. Stoddart, *Angew. Chem., Int. Ed.*, 2012, **51**, 12902–12903.
2. S. Srinivasan, V. K. Praveen, R. Philip, and A. Ajayaghosh, *Angew. Chem., Int. Ed.*, 2008, **47**, 5750–5754.
3. R. J. Williams, A. M. Smith, R. Collins, N. Hodson, A. K. Das, and R. V. Ulijn, *Nat. Nanotechnol.*, 2009, **4**, 19–24.
4. R. J. Williams, R. J. Mart, and R. V. Ulijn, *Biopolymers*, 2010, **94**, 107–117.
5. B. Adhikari and B. Arindam, *J. Indian Inst. Sci.*, 2011, **91**, 471–483.
6. K. J. Skilling, F. Citossi, T. D. Bradshaw, M. Ashford, B. Kellam, and M. Marlow, *Soft Matter*, 2014, **10**, 237–256.
7. S. S. Babu, V. K. Praveen, and A. Ajayaghosh, *Chem. Rev.*, 2014, **114**, 1973–2129.
8. G. Fichman and E. Gazit, *Acta Biomater.*, 2014, **10**, 1671–1682.
9. D. J. Adams, *Macromol. Biosci.*, 2011, **11**, 160–173.
10. D. M. Ryan and B. L. Nilsson, *Polym. Chem.*, 2012, **3**, 18–33.
11. T. Aida, E. W. Meijer, and S. I. Stupp, *Science*, 2012, **335**, 813–817.

12. L. A. Estroff and A. D. Hamilton, *Chem. Rev.*, 2004, **104**, 1201–1218.
13. L. Yu and J. Ding, *Chem. Soc. Rev.*, 2008, **37**, 1473–1481.
14. M. C. Branco and J. P. Schneider, *Acta Biomater.*, 2009, **5**, 817–831.
15. C. Y. Xu and J. Kopecek, *Polym. Bull.*, 2007, **58**, 53–63.
16. B. O. Okesola and D. K. Smith, *Chem. Commun.*, 2013, **49**, 11164–11166.
17. D. K. Smith, *Nat. Chem.*, 2010, **2**, 162–163.
18. N. A. Dudukovic and C. F. Zukoski, *Langmuir*, 2014, **30**, 4493–4500.
19. P. W. J. M. Frederix, R. Kania, J. A. Wright, D. A. Lamprou, R. Ulijn, C. J. Pickett, and N. T. Hunt, *Dalton Trans.*, 2012, **41**, 13112–13119.
20. B. Escuder, F. Rodríguez-Llansola, and J. F. Miravet, *New J. Chem.*, 2010, **34**, 1044–1054.
21. Y. Gao, F. Zhao, Q. Wang, Y. Zhang, and B. Xu, *Chem. Soc. Rev.*, 2010, **39**, 3425–3433.
22. Z. Huang, S. Guan, Y. Wang, G. Shi, L. Cao, Y. Gao, Z. Dong, J. Xu, Q. Luo, and J. Liu, *J. Mater. Chem. B*, 2013, **1**, 2297–2304.
23. G. Scott, S. Roy, Y. M. Abul-Haija, S. Fleming, S. Bai, and R. V. Ulijn, *Langmuir*, 2013, **29**, 14321–14327.
24. R. Huang, S. Wu, A. Li, and Z. Li, *J. Mater. Chem. A*, 2014, **2**, 1672–1676.
25. X. Yan, P. Zhu, and J. Li, *Chem. Soc. Rev.*, 2010, **39**, 1877–1890.
26. M. Reches and E. Gazit, *Science*, 2003, **300**, 625–627.
27. B. Adhikari and A. Banerjee, *Chem. - Eur. J.*, 2010, **16**, 13698–13705.
28. S. Roy and A. Banerjee, *Soft Matter*, 2011, **7**, 5300–5308.
29. L. S. Birchall, R. V. Ulijn, and S. J. Webb, *Chem. Commun.*, 2008, 2861–2863.
30. Z. Yang and B. Xu, *Chem. Commun.*, 2004, 2424–2425.
31. Z. Yang, P.-L. Ho, G. Liang, K. H. Chow, Q. Wang, Y. Cao, Z. Guo, and B. Xu, *J. Am. Chem. Soc.*, 2007, **129**, 266–267.
32. A. Richter, G. Paschew, S. Klatt, J. Lienig, K.-F. Arndt, and H.-J. P. Adler, *Sensors*, 2008, **8**, 561–581.
33. S. Debnath, A. Shome, D. Das, and P. K. Das, *J. Phys. Chem. B*, 2010, **114**, 4407–4415.
34. Y. Gao, Y. Kuang, Z.-F. Guo, Z. Guo, I. J. Krauss, and B. Xu, *J. Am. Chem. Soc.*, 2009, **131**, 13576–13577.
35. G. Liang, Z. Yang, R. Zhang, L. Li, Y. Fan, Y. Kuang, Y. Gao, T. Wang, W. W. Lu, and B. Xu, *Langmuir*, 2009, **25**, 8419–8422.
36. Y. Zhang, H. Gu, Z. Yang, and B. Xu, *J. Am. Chem. Soc.*, 2003, **125**, 13680–13681.
37. A. Mahler, M. Reches, M. Rechter, S. Cohen, and E. Gazit, *Adv. Mater.*, 2006, **18**, 1365–1366.
38. J. Nanda and A. Banerjee, *Soft Matter*, 2012, **8**, 3380–3386.
39. Y. Wang, W. Qi, R. Huang, R. Su, and Z. He, *RSC Adv.*, 2014, **4**, 15340–15347.
40. S. Maity, S. Nir, and M. Reches, *J. Mater. Chem. B*, 2014, **2**, 2583–2591.
41. S. Bai, C. Pappas, S. Debnath, P. W. J. M. Frederix, J. Leckie, S. Fleming, and R. V. Ulijn, *ACS Nano*, 2014, **8**, 7005–7013.
42. M. Zhou, A. M. Smith, A. K. Das, N. W. Hodson, R. F. Collins, R. V. Ulijn, and J. E. Gough, *Biomaterials*, 2009, **30**, 2523–2530.
43. V. Jayawarna, S. M. Richardson, A. R. Hirst, N. W. Hodson, A. Saiani, J. E. Gough, and R. V. Ulijn, *Acta Biomater.*, 2009, **5**, 934–943.
44. Z. Yang, G. Liang, M. Ma, Y. Gao, and B. Xu, *Small*, 2007, **3**, 558–562.
45. Z. Yang, G. Liang, L. Wang, and B. Xu, *J. Am. Chem. Soc.*, 2006, **128**, 3038–3043.
46. G. Cheng, V. Castelletto, R. R. Jones, C. J. Connon, and I. W. Hamley, *Soft Matter*, 2011, **7**, 1326–1333.
47. V. N. Modepalli, A. L. Rodriguez, R. Li, S. Pavuluri, K. R. Nicholas, C. J. Barrow, D. R. Nisbet, and R. J. Williams, *Biopolymers*, 2014, **102**, 197–205.
48. E. Winfree, F. Liu, L. A. Wenzler, and N. C. Seeman, *Nature*, 1998, **394**, 539–544.
49. S. M. Douglas, H. Dietz, T. Liedl, B. Högberg, F. Graf, and W. M. Shih, *Nature*, 2009, **459**, 414–418.
50. X. Li, Y. Kuang, H.-C. Lin, Y. Gao, J. Shi, and B. Xu, *Angew. Chem., Int. Ed.*, 2011, **50**, 9365–9369.
51. L. S. Birchall, S. Roy, V. Jayawarna, M. Hughes, E. Irvine, G. T. Okorogheye, N. Saudi, E. D. Santis, T. Tuttle, A. A. Edwards, and R. V. Ulijn, *Chem. Sci.*, 2011, **2**, 1349–1355.
52. R. Roytman, L. Adler-Abramovich, K. S. A. Kumar, T.-C. Kuan, C.-C. Lin, E. Gazit, and A. Brik, *Org. Biomol. Chem.*, 2011, **9**, 5755–5761.
53. N. Gour, A. K. Barman, and S. Verma, *J. Pept. Sci.*, 2012, **18**, 405–412.
54. M. Mahato, V. Arora, R. Pathak, H. K. Gautam, and A. K. Sharma, *Mol. BioSyst.*, 2012, **8**, 1742–1749.
55. L. Liu, K. Busuttil, S. Zhang, Y. Yang, C. Wang, F. Besenbacher, and M. Dong, *Phys. Chem. Chem. Phys.*, 2011, **13**, 17435–17444.
56. A. Petrov and G. F. Audette, *Wiley Interdiscip. Rev.: Nanomed. Nanobiotechnol.*, 2012, **4**, 575–585.
57. R. V. Ulijn and A. M. Smith, *Chem. Soc. Rev.*, 2008, **37**, 664–675.
58. H. Wang, Z. Yang, and D. J. Adams, *Mater. Today*, 2012, **15**, 500–507.
59. E. Gazit, *Chem. Soc. Rev.*, 2007, **36**, 1263–1269.
60. J. B. Matson and S. I. Stupp, *Chem. Commun.*, 2012, **48**, 26–33.
61. S. Zhang and X. Zhao, *J. Mater. Chem.*, 2004, **14**, 2082–2086.
62. J. T. Pelton and L. R. McLean, *Anal. Biochem.*, 2000, **277**, 167–176.
63. F. Eisenhaber, B. Persson, and P. Argos, *Crit. Rev. Biochem. Mol. Biol.*, 1995, **30**, 1–94.
64. N. J. Greenfield, *Nat. Protoc.*, 2006, **1**, 2876–2890.
65. S. Toksöz and M. O. Guler, *Nano Today*, 2009, **4**, 458–469.
66. M. Biancalana, K. Makabe, A. Koide, and S. Koide, *J. Mol. Biol.*, 2008, **383**, 205–213.
67. R. V. Ulijn and D. N. Woolfson, *Chem. Soc. Rev.*, 2010, **39**, 3349–3350.
68. J. M. Fletcher, R. L. Harniman, F. R. H. Barnes, A. L. Boyle, A. Collins, J. Mantell, T. H. Sharp, M. Antognozzi, P. J. Booth, N. Linden, M. J. Miles, R. B. Sessions, P. Verkade, and D. N. Woolfson, *Science*, 2013, **340**, 595–599.
69. W. F. DeGrado and J. D. Lear, *J. Am. Chem. Soc.*, 1985, **107**, 7684–7689.
70. L. E. R. O'Leary, J. A. Fallas, E. L. Bakota, M. K. Kang, and J. D. Hartgerink, *Nat. Chem.*, 2011, **3**, 821–828.
71. A. V. Persikov, J. A. M. Ramshaw, A. Kirkpatrick, and B. Brodsky, *Biochemistry*, 2000, **39**, 14960–14967.
72. D. W. Urry and M. M. Long, *CRC Crit. Rev. Biochem.*, 1976, **4**, 1–45.
73. D. E. Meyer and A. Chilkoti, *Biomacromolecules*, 2004, **5**, 846–851.
74. L. Ayres, K. Koch, and J. C. M. van Hest, *Macromolecules*, 2005, **38**, 1699–1704.
75. J. Naskar, G. Palui, and A. Banerjee, *J. Phys. Chem. B*, 2009, **113**, 11787–11792.
76. S. Perween, B. Chandanshive, H. C. Kotamarthi, and D. Khushalani, *Soft Matter*, 2013, **9**, 10141–10145.
77. L. Zang, Y. K. Che, and J. S. Moore, *Acc. Chem. Res.*, 2008, **41**, 1596–1608.
78. S. R. Diegelmann, J. M. Gorham, and J. D. Tovar, *J. Am. Chem. Soc.*, 2008, **130**, 13840–13841.
79. W.-W. Tsai, I. D. Tevis, A. S. Tayi, H. Cui, and S. I. Stupp, *J. Phys. Chem. B.*, 2010, **114**, 14778–14786.
80. M. O. Guler, R. C. Claussen, and S. I. Stupp, *J. Mater. Chem.*, 2005, **15**, 4507–4512.
81. A. Brizard, M. Stuart, K. van Bommel, A. Friggeri, M. de Jong, and J. van Esch, *Angew. Chem., Int. Ed.*, 2008, **47**, 2063–2066.
82. G. S. Vadehra, B. D. Wall, S. R. Diegelmann, and J. D. Tovar, *Chem. Commun.*, 2010, **46**, 3947–3949.
83. P. Dastidar, *Chem. Soc. Rev.*, 2008, **37**, 2699–2715.
84. C. Subbalakshmi, S. V. Manorama, and R. Nagaraj, *J. Pept. Sci.*, 2012, **18**, 283–292.
85. V. Castelletto, G. Cheng, C. Stain, C. J. Connon, and I. W. Hamley, *Langmuir*, 2012, **28**, 11599–11608.
86. V. Castelletto, G. Cheng, B. W. Greenland, I. W. Hamley, and P. J. F. Harris, *Langmuir*, 2011, **27**, 2980–2988.
87. G. Palui, J. Nanda, S. Ray, and A. Banerjee, *Chem. - Eur. J.*, 2009, **15**, 6902–6909.

88. B. Adhikari, G. Palui, and A. Banerjee, *Soft Matter*, 2009, **5**, 3452–3460.
89. J. Nanda, B. Adhikari, S. Basak, and A. Banerjee, *J. Phys. Chem. B*, 2012, **116**, 12235–12244.
90. S. Debnath, A. Shome, S. Dutta, and P. K. Das, *Chem. - Eur. J.*, 2008, **14**, 6870–6881.
91. T. Kar, S. Dutta, and P. K. Das, *Soft Matter*, 2010, **6**, 4777–4787.
92. A. Shome, S. Dutta, S. Maiti, and P. K. Das, *Soft Matter*, 2011, **7**, 3011–3022.
93. S. K. Mandal, T. Kar, D. Das, and P. K. Das, *Chem. Commun.*, 2012, **48**, 1814–1816.
94. R. N. Mitra, D. Das, S. Roy, and P. K. Das, *J. Phys. Chem. B*, 2007, **111**, 14107–14113.
95. T. Kar, S. Debnath, D. Das, A. Shome, and P. Das, *Langmuir*, 2009, **25**, 8639–8648.
96. S. Yuran, Y. Razvag, and M. Reches, *ACS Nano*, 2012, **6**, 9559–9566.
97. R. N. Mitra, A. Shome, P. Paul, and P. K. Das, *Org. Biomol. Chem.*, 2009, **7**, 94–102.
98. R. Solaro, M. Alderighi, M. C. Barsotti, A. Battisti, M. Cifelli, P. Losi, R. D. Stefano, L. Ghezzi, and M. R. Tiné, *J. Bioact. Compat. Polym.*, 2013, **28**, 3–15.
99. A. Dehsorkhi, I. W. Hamley, J. Seitsonen, and J. Ruokolainen, *Langmuir*, 2013, **29**, 6665–6672.
100. C. Berdugo, J. F. Miravet, and B. Escuder, *Chem. Commun.*, 2013, **49**, 10608–10610.
101. S. Cavalli, F. Albericio, and A. Kros, *Chem. Soc. Rev.*, 2010, **39**, 241–263.
102. H. G. Cui, M. J. Webber, and S. I. Stupp, *Biopolymers*, 2010, **94**, 1–18.
103. F. Versluis, H. R. Marsden, and A. Kros, *Chem. Soc. Rev.*, 2010, **39**, 3434–3444.
104. I. W. Hamley, *Soft Matter*, 2011, **7**, 4122–4138.
105. D. J. Adams and P. D. Topham, *Soft Matter*, 2010, **6**, 3707–3721.
106. A. L. Boyle and D. N. Woolfson, *Chem. Soc. Rev.*, 2011, **40**, 4295–4306.
107. M. Zelzer and R. V. Ulijn, *Chem. Soc. Rev.*, 2010, **39**, 3351–3357.
108. S. Fleming, S. Debnath, P. W. J. M. Frederix, T. Tuttle, and R. V. Ulijn, *Chem. Commun.*, 2013, **49**, 10587–10589.
109. D. M. Ryan, T. M. Doran, S. B. Anderson, and B. L. Nilsson, *Langmuir*, 2011, **27**, 4029–4039.
110. M. Hughes, H. Xu, P. W. J. M. Frederix, A. M. Smith, N. T. Hunt, T. Tuttle, I. A. Kinloch, and R. V. Ulijn, *Soft Matter*, 2011, **7**, 10032–10038.
111. H. Shao and J. R. Parquette, *Chem. Commun.*, 2010, **46**, 4285–4287.
112. L. Chen, K. Morris, A. Laybourn, D. Elias, M. R. Hicks, A. Rodger, L. Serpell, and D. J. Adams, *Langmuir*, 2010, **26**, 5232–5242.
113. R. Orbach, I. Mironi-Harpaz, L. Adler-Abramovich, E. Mossou, E. P. Mitchell, V. T. Forsyth, E. Gazit, and D. Seliktar, *Langmuir*, 2012, **28**, 2015–2022.
114. A. R. Hirst, S. Roy, M. Arora, A. K. Das, N. Hodson, P. Murray, S. Marshall, N. Javid, J. Sefcik, J. Boekhoven, J. H. van Esch, S. Santabarbara, N. T. Hunt, and R. V. Ulijn, *Nat. Chem.*, 2010, **2**, 1089–1094.
115. A. M. Smith, R. F. Collins, R. V. Ulijn, and E. Blanch, *J. Raman Spectrosc.*, 2009, **40**, 1093–1095.
116. S. Fleming, P. W. J. M. Frederix, I. Ramos-Sasselli, N. Hunt, R. V. Ulijn, and T. Tuttle, *Langmuir*, 2013, **29**, 9510–9515.
117. J. D. Hartgerink, E. Beniash, and S. I. Stupp, *Proc. Natl. Acad. Sci. U. S. A.*, 2002, **99**, 5133–5138.
118. E. Beniash, J. D. Hartgerink, H. Storrie, J. C. Stendahl, and S. I. Stupp, *Acta Biomater.*, 2005, **1**, 387–397.
119. A. Ohta, M. Shirai, T. Asakawa, and S. Miyagishi, *J. Oleo Sci.*, 2008, **57**, 659–667.
120. S. Dutta, A. Shome, S. Debnath, and P. K. Das, *Soft Matter*, 2009, **5**, 1607–1620.
121. E. T. Pashuck and S. I. Stupp, *J. Am. Chem. Soc.*, 2010, **132**, 8819–8820.
122. S. M. Standley, D. J. Toft, H. Cheng, S. Soukasene, J. Chen, S. M. Raja, V. Band, H. Band, V. L. Cryns, and S. I. Stupp, *Cancer Res.*, 2010, **70**, 3020–3026.
123. A. Pal and J. Dey, *Soft Matter*, 2011, **7**, 10369–10376.
124. A. Tan, J. Rajadas, and A. M. Seifalian, *J. Controlled Release*, 2012, **163**, 342–352.
125. C. R. Martinez and B. L. Iverson, *Chem. Sci.*, 2012, **3**, 2191–2201.
126. H. Wang, C. Yang, M. Tan, L. Wang, D. Kong, and Z. Yang, *Soft Matter*, 2011, **7**, 3897–3905.
127. C. Tang, R. V. Ulijn, and A. Saiani, *Langmuir*, 2011, **27**, 14438–14449.
128. L. Chen, S. Revel, K. Morris, L. C. Serpell, and D. J. Adams, *Langmuir*, 2010, **26**, 13466–13471.
129. M. Hughes, P. W. J. M. Frederix, J. Raeburn, L. S. Birchall, J. Sadownik, F. C. Coomer, I.-H. Lin, E. J. Cussen, N. T. Hunt, T. Tuttle, S. J. Webb, D. J. Adams, and R. V. Ulijn, *Soft Matter*, 2012, **8**, 5595–5602.
130. Z. Yang, G. Liang, M. Ma, Y. Gao, and B. Xu, *J. Mater. Chem.*, 2007, **17**, 850–854.
131. D. J. Adams, L. M. Mullen, M. Berta, L. Chen, and W. J. Frith, *Soft Matter*, 2010, **6**, 1971–1980.
132. D. M. Ryan, S. B. Anderson, and B. L. Nilsson, *Soft Matter*, 2010, **6**, 3220–3231.
133. R. Orbach, L. Adler-Abramovich, S. Zigerson, I. Mironi-Harpaz, D. Seliktar, and E. Gazit, *Biomacromolecules*, 2009, **10**, 2646–2651.
134. Y. Huang, Z. Qiu, Y. Xu, J. Shi, H. Lin, and Y. Zhang, *Org. Biomol. Chem.*, 2011, **9**, 2149–2155.
135. J. Raeburn, A. Z. Cardoso, and D. J. Adams, *Chem. Soc. Rev.*, 2013, **42**, 5143–5156.
136. R. Vegners, I. Shestakova, I. Kalvinsh, R. M. Ezzell, and P. A. Janmey, *J. Pept. Sci.*, 1995, **1**, 371–378.
137. Z. Yang, H. Gu, Y. Zhang, L. Wang, and B. Xu, *Chem. Commun.*, 2004, 208–209.
138. Y. Zhang, Z. Yang, F. Yuan, H. Gu, P. Gao, and B. Xu, *J. Am. Chem. Soc.*, 2004, **126**, 15028–15029.
139. Z. Yang, H. Gu, D. Fu, P. Gao, J. K. Lam, and B. Xu, *Adv. Mater.*, 2004, **16**, 1440–1444.
140. M. J. Krysmann, V. Castelletto, A. Kelarakis, I. W. Hamley, R. A. Hule, and D. J. Pochan, *Biochemistry*, 2008, **47**, 4597–4605.
141. E. Gazit, *Prion*, 2007, **1**, 32–35.
142. P. Tamamis, L. Adler-Abramovich, M. Reches, K. Marshall, P. Sikorski, L. Serpell, E. Gazit, and G. Archontis, *Biophys. J.*, 2009, **96**, 5020–5029.
143. M. J. Krysmann, V. Castelletto, J. E. McKendrick, L. A. Clifton, I. W. Hamley, P. J. F. Harris, and S. A. King, *Langmuir*, 2008, **24**, 8158–8162.
144. N. S. de Groot, T. Parella, F. X. Aviles, J. Vendrell, and S. Ventura, *Biophys. J.*, 2007, **92**, 1732–1741.
145. S. Marchesan, C. D. Easton, F. Kushkaki, L. Waddington, and P. G. Hartley, *Chem. Commun.*, 2012, **48**, 2195–2197.
146. C. H. Görbitz, *Chem. Commun.*, 2006, 2332–2334.
147. L. Adler-Abramovich, M. Reches, V. L. Sedman, S. Allen, S. J. B. Tendler, and E. Gazit, *Langmuir*, 2006, **22**, 1313–1320.
148. M. Reches and E. Gazit, *Phys. Biol.*, 2006, **3**, S10–S19.
149. L. Adler-Abramovich, L. Vaks, O. Carny, D. Trudler, A. Magno, A. Caflisch, D. Frenkel, and E. Gazit, *Nat. Chem. Biol.*, 2012, **8**, 701–706.
150. E. Gazit, *FASEB J.*, 2002, **16**, 77–83.
151. M. Reches, Y. Porat, and E. Gazit, *J. Biol. Chem.*, 2002, **277**, 35475–35480.
152. M. Reches and E. Gazit, *Nano Lett.*, 2004, **4**, 581–585.
153. M. Reches and E. Gazit, *Isr. J. Chem.*, 2005, **45**, 363–371.
154. V. Jayawarna, M. Ali, T. A. Jowitt, A. E. Miller, A. Saiani, J. E. Gough, and R. V. Ulijn, *Adv. Mater.*, 2006, **18**, 611–612.
155. Z. A. C. Schnepp, R. Gonzalez-McQuire, and S. Mann, *Adv. Mater.*, 2006, **18**, 1869–1872.
156. Z. Yang and B. Xu, *Adv. Mater.*, 2006, **18**, 3043–3046.
157. Z. Yang, G. Liang, and B. Xu, *Chem. Commun.*, 2006, 738–740.
158. S. Toledano, R. J. Williams, V. Jayawarna, and R. V. Ulijn, *J. Am. Chem. Soc.*, 2006, **128**, 1070–1071.
159. V. Jayawarna, A. Smith, J. E. Gough, and R. V. Ulijn, *Biochem. Soc. Trans.*, 2007, **35**, 535–537.
160. Z. Yang and B. Xu, *J. Mater. Chem.*, 2007, **17**, 2385–2393.
161. L. Adler-Abramovich and E. Gazit, *J. Pept. Sci.*, 2008, **14**, 217–223.

162. D. Bardelang, M. B. Zaman, I. L. Moudrakovski, S. Pawsey, J. C. Margeson, D. S. Wang, X. H. Wu, J. A. Ripmeester, C. I. Ratcliffe, and K. Yu, *Adv. Mater.*, 2008, **20**, 4517–4520.
163. A. K. Das, R. Collins, and R. V. Ulijn, *Small*, 2008, **4**, 279–287.
164. A. M. Smith, R. J. Williams, C. Tang, P. Coppo, R. F. Collins, M. L. Turner, A. Saiani, and R. V. Ulijn, *Adv. Mater.*, 2008, **20**, 37–41.
165. Z. Yang, G. Liang, and B. Xu, *Acc. Chem. Res.*, 2008, **41**, 315–326.
166. D. J. Adams, M. F. Butler, W. J. Frith, M. Kirkland, L. Mullen, and P. Sanderson, *Soft Matter*, 2009, **5**, 1856–1862.
167. A. K. Das, A. R. Hirst, and R. V. Ulijn, *Faraday Discuss.*, 2009, **143**, 293–303.
168. J. Gao, H. Wang, L. Wang, J. Wang, D. Kong, and Z. Yang, *J. Am. Chem. Soc.*, 2009, **131**, 11286–11287.
169. H. Shao, T. Nguyen, N. C. Romano, D. A. Modarelli, and J. R. Parquette, *J. Am. Chem. Soc.*, 2009, **131**, 16374–16376.
170. K. Thornton, A. M. Smith, C. L. R. Merry, and R. V. Ulijn, *Biochem. Soc. Trans.*, 2009, **37**, 660–664.
171. C. Tang, A. M. Smith, R. F. Collins, R. V. Ulijn, and A. Saiani, *Langmuir*, 2009, **25**, 9447–9453.
172. S. Sutton, N. L. Campbell, A. I. Cooper, M. Kirkland, W. J. Frith, and D. J. Adams, *Langmuir*, 2009, **25**, 10285–10291.
173. D. J. Adams, K. Morris, L. Chen, L. C. Serpell, J. Bacsa, and G. M. Day, *Soft Matter*, 2010, **6**, 4144–4156.
174. N. Amdursky, E. Gazit, and G. Rosenman, *Adv. Mater.*, 2010, **22**, 2311–2315.
175. L. Chen, S. Revel, K. Morris, and D. J. Adams, *Chem. Commun.*, 2010, **46**, 4267–4269.
176. L. Chen, S. Revel, K. Morris, D. G. Spiller, L. C. Serpell, and D. J. Adams, *Chem. Commun.*, 2010, **46**, 6738–6740.
177. G. Cheng, V. Castelletto, C. M. Moulton, G. E. Newby, and I. W. Hamley, *Langmuir*, 2010, **26**, 4990–4998.
178. E. K. Johnson, D. J. Adams, and P. J. Cameron, *J. Am. Chem. Soc.*, 2010, **132**, 5130–5136.
179. M. L. Ma, Y. Kuang, Y. Gao, Y. Zhang, P. Gao, and B. Xu, *J. Am. Chem. Soc.*, 2010, **132**, 2719–2728.
180. D. M. Ryan, S. B. Anderson, F. T. Senguen, R. E. Youngman, and B. L. Nilsson, *Soft Matter*, 2010, **6**, 475–479.
181. D. M. Ryan, T. M. Doran, and B. L. Nilsson, *Chem. Commun.*, 2010, **47**, 475–477.
182. J. Ryu, S.-W. Kim, K. Kang, and C. B. Park, *Adv. Mater.*, 2010, **22**, 5537–5541.
183. J. W. Sadownik, J. Leckie, and R. V. Ulijn, *Chem. Commun.*, 2010, **47**, 728–730.
184. J. W. Sadownik and R. V. Ulijn, *Chem. Commun.*, 2010, **46**, 3481–3483.
185. H. X. Xu, A. K. Das, M. Horie, M. S. Shaik, A. M. Smith, Y. Luo, X. F. Lu, R. Collins, S. Y. Liem, A. M. Song, P. L. A. Popelier, M. L. Turner, P. Xiao, I. A. Kinloch, and R. V. Ulijn, *Nanoscale*, 2010, **2**, 960–966.
186. X.-D. Xu, C.-S. Chen, B. Lu, S.-X. Cheng, X.-Z. Zhang, and R.-X. Zhuo, *J. Phys. Chem. B*, 2010, **114**, 2365–2372.
187. Z. Yang, L. Wang, J. Wang, P. Gao, and B. Xu, *J. Mater. Chem.*, 2010, **20**, 2128–2132.
188. B. Adhikari and A. Banerjee, *Soft Matter*, 2011, **7**, 9259–9266.
189. B. Adhikari, J. Nanda, and A. Banerjee, *Soft Matter*, 2011, **7**, 8913–8922.
190. L. Chen, G. Pont, K. Morris, G. Lotze, A. Squires, L. C. Serpell, and D. J. Adams, *Chem. Commun.*, 2011, **47**, 12071–12073.
191. L. Chen, J. Raeburn, S. Sutton, D. G. Spiller, J. Williams, J. S. Sharp, P. C. Griffiths, R. K. Heenan, S. M. King, A. Paul, S. Furzeland, D. Atkins, and D. J. Adams, *Soft Matter*, 2011, **7**, 9721–9727.
192. W. Helen, P. de Leonardis, R. V. Ulijn, J. Gough, and N. Tirelli, *Soft Matter*, 2011, **7**, 1732–1740.
193. M. Ikeda, T. Tanida, T. Yoshii, and I. Hamachi, *Adv. Mater.*, 2011, **23**, 2819–2822.
194. E. K. Johnson, D. J. Adams, and P. J. Cameron, *J. Mater. Chem.*, 2011, **21**, 2024–2027.
195. T. Kar, S. K. Mandal, and P. K. Das, *Chem. - Eur. J.*, 2011, **17**, 14952–14961.
196. Y. Lin, Y. Qiao, P. Tang, Z. Li, and J. Huang, *Soft Matter*, 2011, **7**, 2762–2769.
197. Y. Liu, E. Kim, R. V. Ulijn, W. E. Bentley, and G. F. Payne, *Adv. Funct. Mater.*, 2011, **21**, 1575–1580.
198. D. M. Ryan, T. M. Doran, and B. L. Nilsson, *Langmuir*, 2011, **27**, 11145–11156.
199. J. Shi, Y. Gao, Z. Yang, and B. Xu, *Beilstein J. Org. Chem.*, 2011, **7**, 167–172.
200. Z.-X. Tie, M. Qin, D.-W. Zou, Y. Cao, and W. Wang, *Chin. Phys. Lett.*, 2011, **28**, 028702.
201. Z. Wang, H. Wang, W. Zheng, J. Zhang, Q. Zhao, S. Wang, Z. Yang, and D. Kong, *Chem. Commun.*, 2011, **47**, 8901–8903.
202. V. Castelletto, C. M. Moulton, G. Cheng, I. W. Hamley, M. R. Hicks, A. Rodger, D. E. López-Pérez, G. Revilla-López, and C. Alemán, *Soft Matter*, 2011, **7**, 11405–11415.
203. H.-G. Braun and A. Z. Cardoso, *Colloids Surf., B*, 2012, **97**, 43–50.
204. M. Hughes, L. S. Birchall, K. Zuberi, L. A. Aitken, S. Debnath, N. Javid, and R. V. Ulijn, *Soft Matter*, 2012, **8**, 11565–11574.
205. D. Jiao, J. Geng, X. J. Loh, D. Das, T.-C. Lee, and O. A. Scherman, *Angew. Chem., Int. Ed.*, 2012, **51**, 9633–9637.
206. D. Li, J. Liu, L. Chu, J. Liu, and Z. Yang, *Chem. Commun.*, 2012, **48**, 6175–6177.
207. X. Mu, K. M. Eckes, M. M. Nguyen, L. J. Suggs, and P. Ren, *Biomacromolecules*, 2012, **13**, 3562–3571.
208. W. Nuansing, A. Rebollo, J. M. Mercero, J. Zuñiga, and A. M. Bittner, *J. Raman Spectrosc.*, 2012, **43**, 1397–1406.
209. J. Raeburn, T. O. McDonald, and D. J. Adams, *Chem. Commun.*, 2012, **48**, 9355–9357.
210. J. Raeburn, G. Pont, L. Chen, Y. Cesbron, R. Lévy, and D. J. Adams, *Soft Matter*, 2012, **8**, 1168–1174.
211. S. Roy, N. Javid, P. W. J. M. Frederix, D. A. Lamprou, A. J. Urquhart, N. T. Hunt, P. J. Halling, and R. V. Ulijn, *Chem. - Eur. J.*, 2012, **18**, 11723–11731.
212. S. Roy, N. Javid, J. Sefcik, P. J. Halling, and R. V. Ulijn, *Langmuir*, 2012, **28**, 16664–16670.
213. S. Roy and A. Banerjee, *RSC Adv.*, 2012, **2**, 2105–2111.
214. C. Tomasini and N. Castellucci, *Chem. Soc. Rev.*, 2012, **42**, 156–172.
215. H. Wang and Z. Yang, *Nanoscale*, 2012, **4**, 5259–5267.
216. L. Chen, T. O. McDonald, and D. J. Adams, *RSC Adv.*, 2013, **3**, 8714–8720.
217. K. L. Morris, L. Chen, J. Raeburn, O. R. Sellick, P. Cotanda, A. Paul, P. C. Griffiths, S. M. King, R. K. O'Reilly, L. C. Serpell, and D. J. Adams, *Nat. Commun.*, 2013, **4**, 1480.
218. S. K. M. Nalluri and R. V. Ulijn, *Chem. Sci.*, 2013, **4**, 3699–3705.
219. K. Thornton, Y. M. Abul-Haija, N. Hodson, and R. Ulijn, *Soft Matter*, 2013, **9**, 9430–9439.
220. M. Hughes, S. Debnath, C. W. Knapp, and R. V. Ulijn, *Biomater. Sci.*, 2013, **1**, 1138–1142.
221. I.-H. Lin, L. S. Birchall, N. Hodson, R. V. Ulijn, and S. J. Webb, *Soft Matter*, 2013, **9**, 1188–1193.
222. J. Li, Y. Kuang, Y. Gao, X. Du, J. Shi, and B. Xu, *J. Am. Chem. Soc.*, 2013, **135**, 542–545.
223. J. Li, X. Li, Y. Kuang, Y. Gao, X. Du, J. Shi, and B. Xu, *Adv. Healthcare Mater.*, 2013, **2**, 1586–1590.
224. Y. Kuang, D. Yuan, Y. Zhang, A. Kao, X. Du, and B. Xu, *RSC Adv.*, 2013, **3**, 7704–7707.
225. J. Li, Y. Kuang, J. Shi, Y. Gao, J. Zhou, and B. Xu, *Beilstein J. Org. Chem.*, 2013, **9**, 908–917.
226. Y. Zhang, R. Zhou, J. Shi, N. Zhou, I. R. Epstein, and B. Xu, *J. Phys. Chem. B*, 2013, **117**, 6566–6573.
227. Y. Kuang and B. Xu, *Angew. Chem., Int. Ed.*, 2013, **52**, 6944–6948.
228. J. Li, Y. Gao, Y. Kuang, J. Shi, X. Du, J. Zhou, H. Wang, Z. Yang, and B. Xu, *J. Am. Chem. Soc.*, 2013, **135**, 9907–9914.
229. C. Ou, J. Zhang, X. Zhang, Z. Yang, and M. Chen, *Chem. Commun.*, 2013, **49**, 1853–1855.
230. J. Majumder, M. R. Das, J. Deb, S. S. Jana, and P. Dastidar, *Langmuir*, 2013, **29**, 10254–10263.
231. S. Debnath, S. Roy, and R. V. Ulijn, *J. Am. Chem. Soc.*, 2013, **135**, 16789–16792.
232. Y. Zou, K. Razmkhah, N. P. Chmel, I. W. Hamley, and A. Rodger, *RSC Adv.*, 2013, **3**, 10854–10858.
233. D. E. López-Pérez, G. Revilla-López, I. W. Hamley, and C. Alemán, *Soft Matter*, 2013, **9**, 11021–11032.

234. H. Zhang, H. Wang, G. Xu, and S. Yuan, *Colloids Surf., A*, 2013, **417**, 217–223.
235. Y. Wang, Z. Zhang, L. Xu, X. Li, and H. Chen, *Colloids Surf., B*, 2013, **104**, 163–168.
236. A. L. Rodriguez, C. L. Parish, D. R. Nisbet, and R. J. Williams, *Soft Matter*, 2013, **9**, 3915–3919.
237. Y. Gao, Y. Kuang, X. Du, J. Zhou, P. Chandran, F. Horkay, and B. Xu, *Langmuir*, 2013, **29**, 15191–15200.
238. Y. Gao, C. Berciu, Y. Kuang, J. Shi, D. Nicastro, and B. Xu, *ACS Nano*, 2013, **7**, 9055–9063.
239. M. Tena-Solsona, J. F. Miravet, and B. Escuder, *Chem. - Eur. J.*, 2014, **20**, 1023–1031.
240. D. Mandal, T. Kar, and P. K. Das, *Chem. - Eur. J.*, 2014, **20**, 1349–1358.
241. S.-M. Hsu, Y.-C. Lin, J.-W. Chang, Y.-H. Liu, and H.-C. Lin, *Angew. Chem., Int. Ed.*, 2014, **53**, 1921–1927.
242. J. T. van Herpt, M. C. A. Stuart, W. R. Browne, and B. L. Feringa, *Chem. - Eur. J.*, 2014, **20**, 3077–3083.
243. S. K. M. Nalluri, C. Berdugo, N. Javid, P. W. J. M. Frederix, and R. V. Ulijn, *Angew. Chem., Int. Ed.*, 2014, **53**, 5882–5887.
244. Y. Kuang, J. Shi, J. Li, D. Yuan, K. A. Alberti, Q. Xu, and B. Xu, *Angew. Chem., Int. Ed.*, 2014, **53**, 8104–8107.
245. S. Fleming, S. Debnath, P. W. J. M. Frederix, N. T. Hunt, and R. V. Ulijn, *Biomacromolecules*, 2014, **15**, 1171–1184.
246. J. Raeburn, B. Alston, J. Kroeger, T. O. McDonald, J. R. Howse, P. J. Cameron, and D. J. Adams, *Mater. Horiz.*, 2014, **1**, 241–246.
247. W. H. Rombouts, M. Giesbers, J. van Lent, F. A. de Wolf, and J. van der Gucht, *Biomacromolecules*, 2014, **15**, 1233–1239.
248. G. Zeng, L. Liu, D. Xia, Q. Li, Z. Xin, J. Wang, F. Besenbacher, T. Skrydstrup, and M. Dong, *RSC Adv.*, 2014, **4**, 7516–7520.
249. M. Caruso, E. Gatto, E. Placidi, G. Ballano, F. Formaggio, C. Toniolo, D. Zanuy, C. Alemán, and M. Venanzi, *Soft Matter*, 2014, **10**, 2508–2519.
250. J. K. Sahoo, S. K. M. Nalluri, N. Javid, H. Webb, and R. V. Ulijn, *Chem. Commun.*, 2014, **50**, 5462–5464.
251. M. M. Nguyen, K. M. Eckes, and L. J. Suggs, *Soft Matter*, 2014, **10**, 2693–2702.
252. J. Zhou, X. Du, Y. Gao, J. Shi, and B. Xu, *J. Am. Chem. Soc.*, 2014, **136**, 2970–2973.
253. K. M. Eckes, X. Mu, M. A. Ruehle, P. Ren, and L. J. Suggs, *Langmuir*, 2014, **30**, 5287–5296.
254. T. Li, M. Kalloudis, A. Z. Cardoso, D. J. Adams, and P. S. Clegg, *Langmuir*, 2014, DOI: 10.1021/la501182t.
255. A. Aufderhorst-Roberts, W. J. Frith, M. Kirkland, and A. M. Donald, *Langmuir*, 2014, **30**, 4483–4492.
256. G. Fichman, L. Adler-Abramovich, S. Manohar, I. Mironi-Harpaz, T. Guterman, D. Seliktar, P. B. Messersmith, and E. Gazit, *ACS Nano*, 2014, **8**, 7220–7228.
257. S. Bai, S. Debnath, K. Gibson, B. Schlicht, L. Bayne, M. Zagnoni, and R. V. Ulijn, *Small*, 2014, **10**, 285–293.
258. Y. M. Abul-Haija, S. Roy, P. W. J. M. Frederix, N. Javid, V. Jayawarna, and R. V. Ulijn, *Small*, 2014, **10**, 973–979.
259. J. H. Kim, D. H. Nam, Y. W. Lee, Y. S. Nam, and C. B. Park, *Small*, 2014, **10**, 1272–1277.
260. Y. Kuang, X. Du, J. Zhou, and B. Xu, *Adv. Healthcare Mater.*, 2014, **3**, 1217–1221.
261. Z. M. Yang, K. M. Xu, Z. F. Guo, Z. H. Guo, and B. Xu, *Adv. Mater.*, 2007, **19**, 3152–3156.
262. Z. Yang, G. Liang, Z. Guo, Z. Guo, and B. Xu, *Angew. Chem., Int. Ed.*, 2007, **46**, 8216–8219.
263. X. Li, X. Du, J. Li, Y. Gao, Y. Pan, J. Shi, N. Zhou, and B. Xu, *Langmuir*, 2012, **28**, 13512–13517.
264. X. Du, J. Zhou, O. Guvench, F. O. Sangiorgi, X. Li, N. Zhou, and B. Xu, *Bioconjugate Chem.*, 2014, **25**, 1031–1035.
265. X. Li, X. Du, Y. Gao, J. Shi, Y. Kuang, and B. Xu, *Soft Matter*, 2012, **8**, 7402–7407.
266. X. Li, Yi Kuang, J. Shi, Y. Gao, H.-C. Lin, and B. Xu, *J. Am. Chem. Soc.*, 2011, **133**, 17513–17518.
267. D. Wu, J. Zhou, J. Shi, X. Du, and B. Xu, *Chem. Commun.*, 2014, **50**, 1992–1994.
268. X. Li, Y. Kuang, and B. Xu, *Soft Matter*, 2012, **8**, 2801–2806.
269. Y. Yamauchi, M. Yoshizawa, and M. Fujita, *J. Am. Chem. Soc.*, 2008, **130**, 5832–5833.
270. K. V. Rao and S. J. George, *Chem. - Eur. J.*, 2012, **18**, 14286–14291.
271. C. Wang, Y. Guo, Z. Wang, and X. Zhang, *Langmuir*, 2010, **26**, 14509–14511.
272. O. P. Lee, A. T. Yiu, P. M. Beaujuge, C. H. Woo, T. W. Holcombe, J. E. Millstone, J. D. Douglas, M. S. Chen, and J. M. J. Fréchet, *Adv. Mater.*, 2011, **23**, 5359–5363.
273. I. Huc and J.-M. Lehn, *Proc. Natl. Acad. Sci. U. S. A.*, 1997, **94**, 2106–2110.
274. J.-M. Lehn, *Chem. - Eur. J.*, 1999, **5**, 2455–2463.
275. O. Ramström and J.-M. Lehn, *Nat. Rev. Drug Discovery*, 2002, **1**, 26–36.
276. P. T. Corbett, J. Leclaire, L. Vial, K. R. West, J.-L. Wietor, J. K. M. Sanders, and S. Otto, *Chem. Rev.*, 2006, **106**, 3652–3711.
277. G. R. Cousins, S.-A. Poulsen, and J. K. Sanders, *Curr. Opin. Chem. Biol.*, 2000, **4**, 270–279.
278. S. Otto, R. L. Furlan, and J. K. Sanders, *Curr. Opin. Chem. Biol.*, 2002, **6**, 321–327.
279. T. Ishi-i, R. Iguchi, E. Snip, M. Ikeda, and S. Shinkai, *Langmuir*, 2001, **17**, 5825–5833.
280. G. D. Rose, A. R. Geselowitz, G. J. Lesser, R. H. Lee, and M. H. Zehfus, *Science*, 1985, **229**, 834–838.
281. R. Cowan and R. G. Whittaker, *Pept. Res.*, 1990, **3**, 75–80.
282. H. Fu, G. R. Grimsley, A. Razvi, J. M. Scholtz, and C. N. Pace, *Proteins: Struct., Funct., Bioinf.*, 2009, **77**, 491–498.
283. M. W. Pantoliano, R. C. Ladner, P. N. Bryan, M. L. Rollence, J. F. Wood, and T. L. Poulos, *Biochemistry*, 1987, **26**, 2077–2082.
284. R. J. Mart, R. D. Osborne, M. M. Stevens, and R. V. Ulijn, *Soft Matter*, 2006, **2**, 822–835.
285. J.-B. Guilbaud, E. Vey, S. Boothroyd, A. M. Smith, R. V. Ulijn, A. Saiani, and A. F. Miller, *Langmuir*, 2010, **26**, 11297–11303.
286. P. W. J. M. Frederix, R. V. Ulijn, N. T. Hunt, and T. Tuttle, *J. Phys. Chem. Lett.*, 2011, **2**, 2380–2384.
287. J. H. van Esch, *Langmuir*, 2009, **25**, 8392–8394.
288. B. Ding, Y. Li, M. Qin, Y. Ding, Y. Cao, and W. Wang, *Soft Matter*, 2013, **9**, 4672–4680.
289. C. Tang, R. V. Ulijn, and A. Saiani, *Eur. Phys. J. E*, 2013, **36**, 111–121.
290. J. Kim, T. H. Han, Y.-I. Kim, J. S. Park, J. Choi, D. G. Churchill, S. O. Kim, and H. Ihee, *Adv. Mater.*, 2010, **22**, 583–587.
291. C. G. Pappas, Y. M. Abul-Haija, A. Flack, P. W. J. M. Frederix, and R. V. Ulijn, *Chem. Commun.*, 2014, **50**, 10630–10633.
292. X.-D. Xu, L. Liang, H. Cheng, X.-H. Wang, F.-G. Jiang, R.-X. Zhuo, and X.-Z. Zhang, *J. Mater. Chem.*, 2012, **22**, 18164–18171.
293. M. A. Greenfield, J. R. Hoffman, M. O. de la Cruz, and S. I. Stupp, *Langmuir*, 2010, **26**, 3641–3647.
294. E. T. Pashuck, H. G. Cui, and S. I. Stupp, *J. Am. Chem. Soc.*, 2010, **132**, 6041–6046.
295. A. Mata, Y. B. Geng, K. J. Henrikson, C. Aparicio, S. R. Stock, R. L. Satcher, and S. I. Stupp, *Biomaterials*, 2010, **31**, 6004–6012.
296. R. N. Shah, N. A. Shah, M. M. D. Lim, C. Hsieh, G. Nuber, and S. I. Stupp, *Proc. Natl. Acad. Sci. U. S. A.*, 2010, **107**, 3293–3298.
297. M. J. Webber, J. Tongers, M. A. Renault, J. G. Roncalli, D. W. Losordo, and S. I. Stupp, *Acta Biomater.*, 2010, **6**, 3–11.
298. H. K. Kang, D. E. Kang, B. H. Boo, S. J. Yoo, J. K. Lee, and E. C. Lim, *J. Phys. Chem. A*, 2005, **109**, 6799–6804.
299. A. Barth and C. Zscherp, *Q. Rev. Biophys.*, 2002, **35**, 369–430.
300. L. Ziserman, H.-Y. Lee, S. R. Raghavan, A. Mor, and D. Danino, *J. Am. Chem. Soc.*, 2011, **133**, 2511–2517.
301. W. Edwards and D. K. Smith, *J. Am. Chem. Soc.*, 2014, **136**, 1116–1124.
302. D. K. Smith, *Chem. Soc. Rev.*, 2009, **38**, 684–694.
303. A. Aggeli, I. A. Nyrkova, M. Bell, R. Harding, L. Carrick, T. C. B. McLeish, A. N. Semenov, and N. Boden, *Proc. Natl. Acad. Sci. U. S. A.*, 2001, **98**, 11857–11862.
304. Y. Gao, J. Shi, D. Yuan, and B. Xu, *Nat. Commun.*, 2012, **3**, 1033.
305. C. Yang, H. Wang, D. Li, and L. Wang, *Chin. J. Chem.*, 2013, **31**, 494–500.
306. F. Hofmeister, *Archiv f. experiment. Pathol. u. Pharmakol.*, 1888, **24**, 247–260.

307.R. V. Ulijn, *J. Mater. Chem.*, 2006, **16**, 2217–2225.
308.M. Zelzer, S. J. Todd, A. R. Hirst, T. O. McDonald, and R. V. Ulijn, *Biomater. Sci.*, 2012, **1**, 11–39.
309.Y. Chen, *Theranostics*, 2012, **2**, 139–147.